Structure functions and large Q^2 cross sections at HERA

Giuseppe Iacobucci
INFN Bologna

- Introduction
- The "transition region" of low Q^2 and x
- F_2 , slopes, QCD fits, F_L and F_2^{charm}
- Large Q^2 NC and CC cross sections
- Summary

Results and Perspectives
in Particle Physics,
La Thuile, February 27 - March 4, 2000

Introduction

$e^{\pm}$ (27.5 GeV) → ← p (820 GeV) 1994-1997

p (920 GeV) 1998-2000

(equivalent to 47-50 TeV fixed target energy)

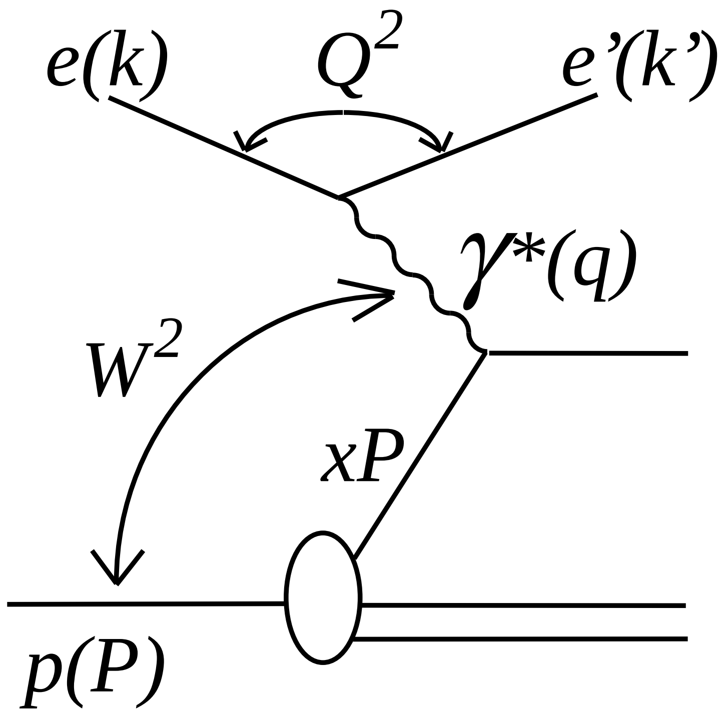

$\sqrt{s} = k + P =$	energy in the ep c.m.s.
$Q^2 = -(k-k')^2 = -q^2 =$	virtuality of the exchanged γ
$x = Q^2/(2P\cdot Q) =$	fraction of proton momentum carried by the struck quark
$y = (P\cdot q)/(P\cdot k) =$	fraction of beam lepton energy transferred to the photon
$W^2 = ys =$	energy in the $\gamma^* p$ c.m.s.
$Q^2 = xys$	

HERA Kinematic Range

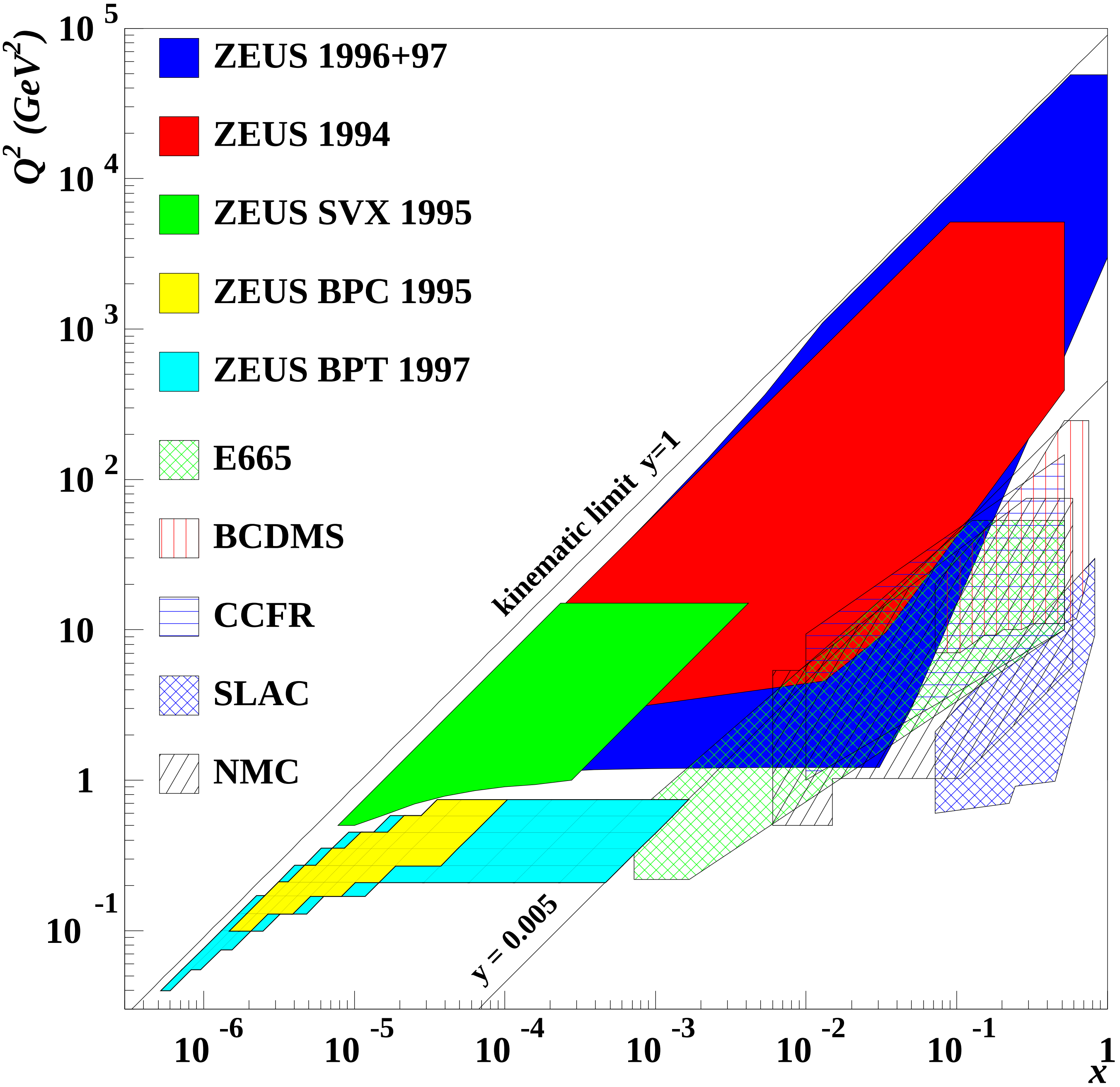

HERA: unique "depth of field" on the proton structure

- Q^2 from ~ 10^{-1} to ~ 10^5 GeV^2
- x down to 10^{-6}

extension by two orders of magnitude both in x and Q^2

F_2 Measurement at HERA

F_2:

High Q^2

Explore new kinematic regions:
where does the Standard Model break down?

Higher and higher precision measurement over a wide kinematic range

Low Q^2

Study the transition from Photoproduction ($Q^2 \cong 0$) to DIS (Q^2 > few GeV^2):
where does pQCD begin to dominate?

We have to precisely measure F_2 to

- **get handle on QCD evolution and**
- **constrain PDF's**

to calculate expected rates at the LHC and estimate neutrino cross sections at ultra-high energies, $E_\nu \sim 10^{12}$ GeV,
in active galactic nuclei, γ-ray bursts

HERA Luminosity

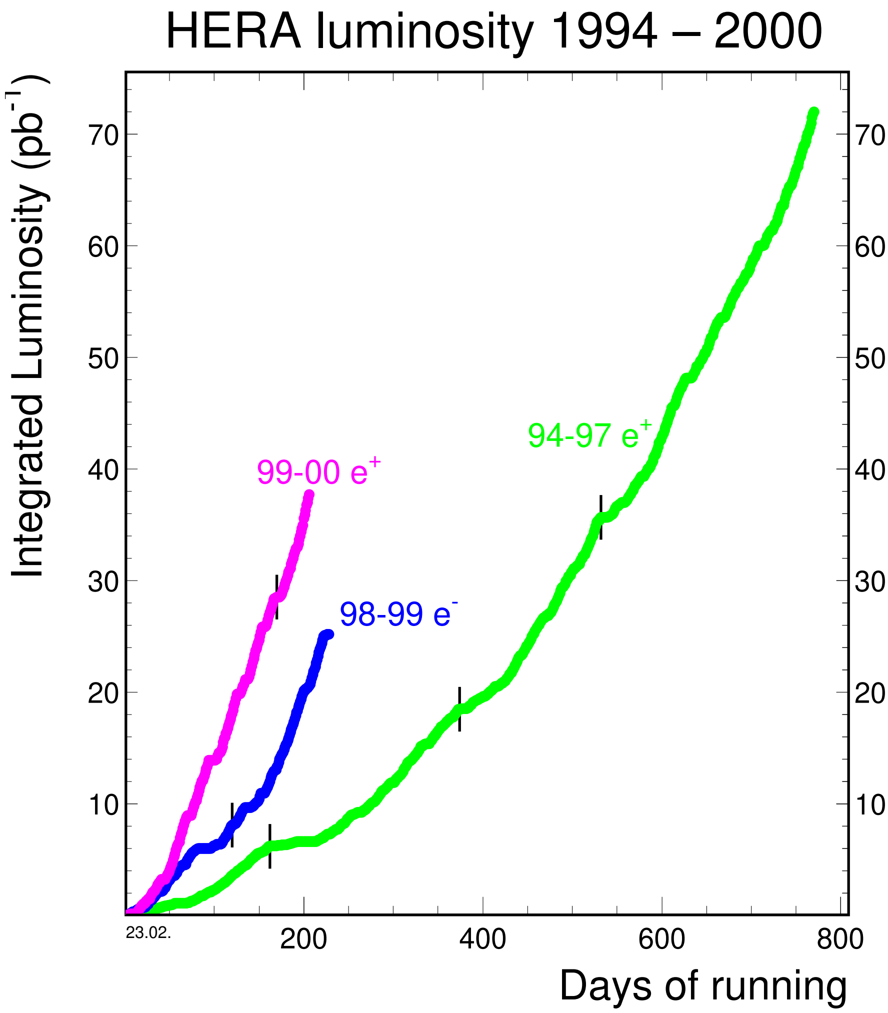

Luminosity available for physics (ZEUS):

1994-97	~ 48 pb^{-1}	e^+p	$\sqrt{s} = 300$ GeV
1998-99	~ 17 pb^{-1}	e^-p	$\sqrt{s} = 320$ GeV
1999-2000	~ 25 pb^{-1}	e^+p	$\sqrt{s} = 320$ GeV
Total	**~ 90 pb^{-1}**		

+ running until September 2000

EW physics at HERA just starting...

The $e^{\pm}p$ Neutral Current Cross Section

$$\frac{d^2\sigma_{NC}^{e^\pm p}}{dx\,dQ^2} = \frac{2\pi\alpha^2}{xQ^4}\cdot \left[Y_+\cdot F_2\left(x,Q^2\right) - y^2 F_L\left(x,Q^2\right) \mp Y_-\cdot xF_3\left(x,Q^2\right)\right]$$

(QED radiative corrections have been neglected)

where:

$$Y_\pm = 1 \pm (1-y)^2$$

quark densities

$$F_2 = x\cdot \sum_{i=quarks} A_i^2\cdot\left(q_i(x) + \bar{q}_i(x)\right)$$

$$xF_3 = x\cdot \sum_{i=quarks} B_i^2\cdot\left(q_i(x) - \bar{q}_i(x)\right),$$ relevant for $Q^2 \approx M_{Z^0}^2$

$$F_L = F_2 - 2xF_1 \cong 0$$ for not too large y

At low Q^2, A_i are the quark electric charges

High precision proton structure at low x-Q^2

- In 1997 ZEUS installed a silicon tracker (BPT) in front of a small calorimeter (BPC) to improve the detection of positrons at small scattered angles

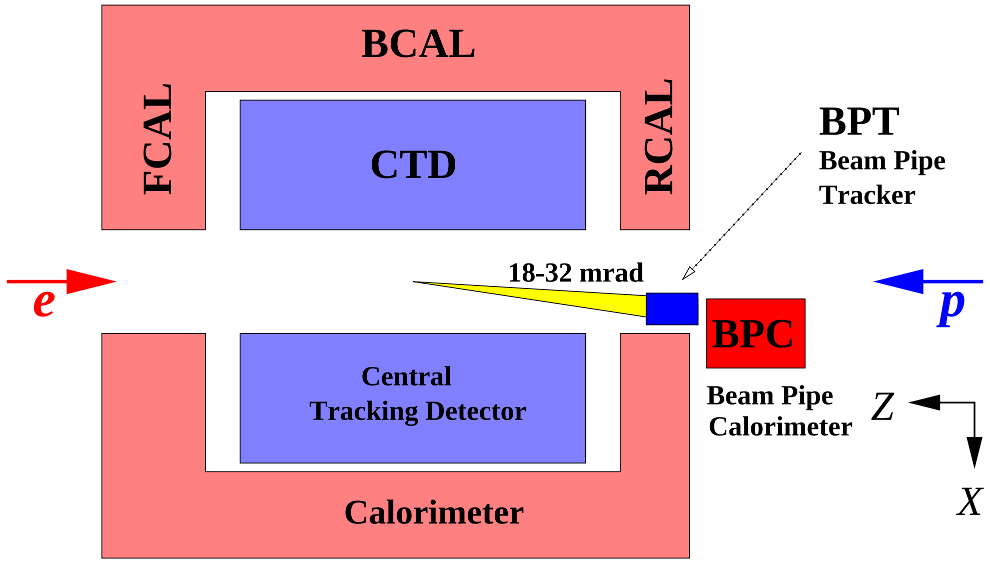

The BPC/T allows F_2 (or $\sigma_{tot}^{\gamma^* p}$) to be measured with high precision in the range:

$$0.045 < Q^2 < 0.65 \text{ GeV}^2$$
$$6 \cdot 10^{-7} < x < 1 \cdot 10^{-3}$$

- 3.9 pb^{-1} collected in 6 weeks during 1997 geometrical acceptance 4-14% depending on the (x,Q^2) bin

- Typical error: $\pm$ 2.6% (stat) $\pm$ 3.3% (syst)

High precision proton structure at low x-Q^2

F_2 values at lowest ever x-Q^2:

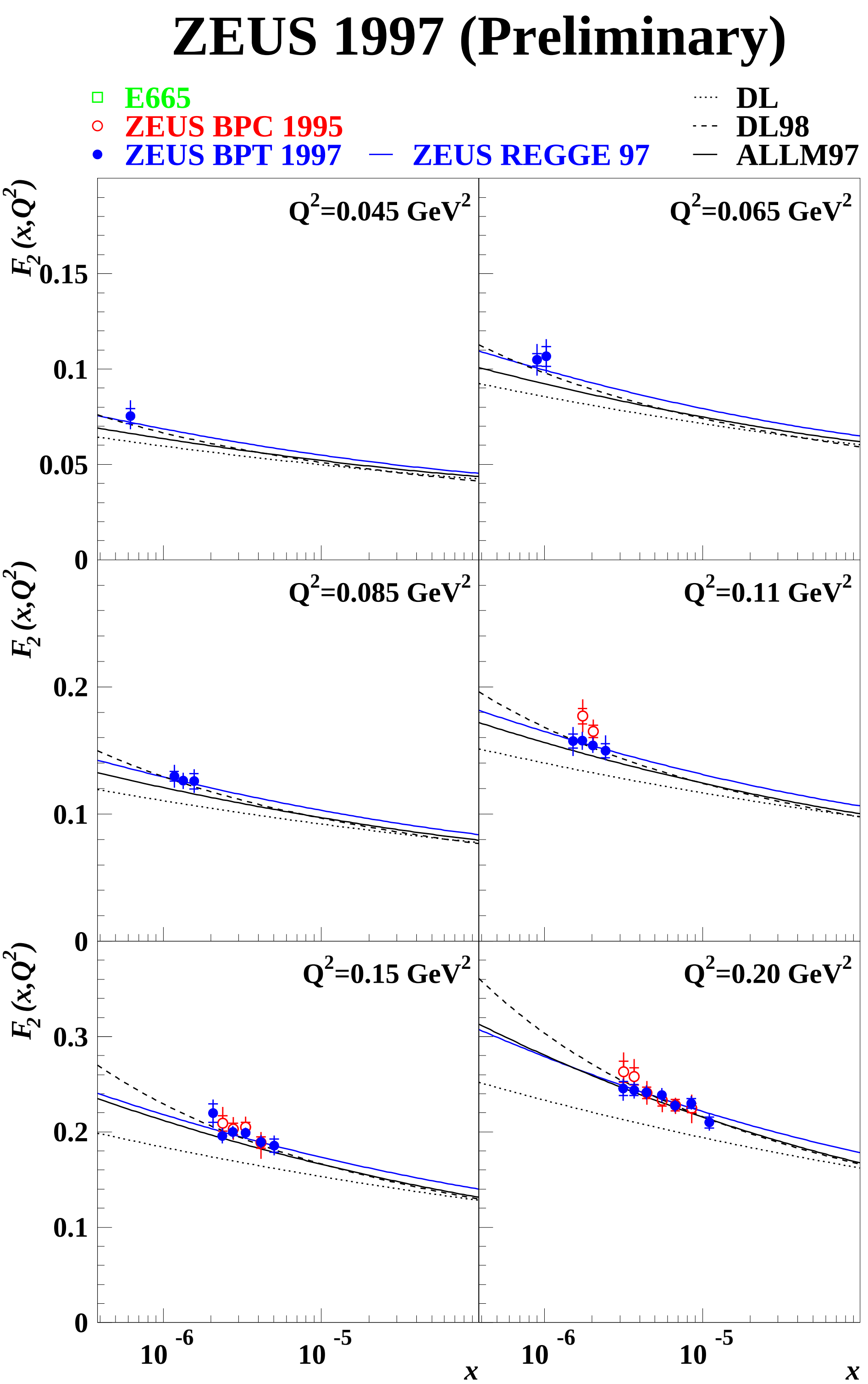

w.r.t. previous ZEUS measurements:

- extension of kinematic range
- higher precision

High precision proton structure at low x-Q^2

ZEUS 1997 (Preliminary)

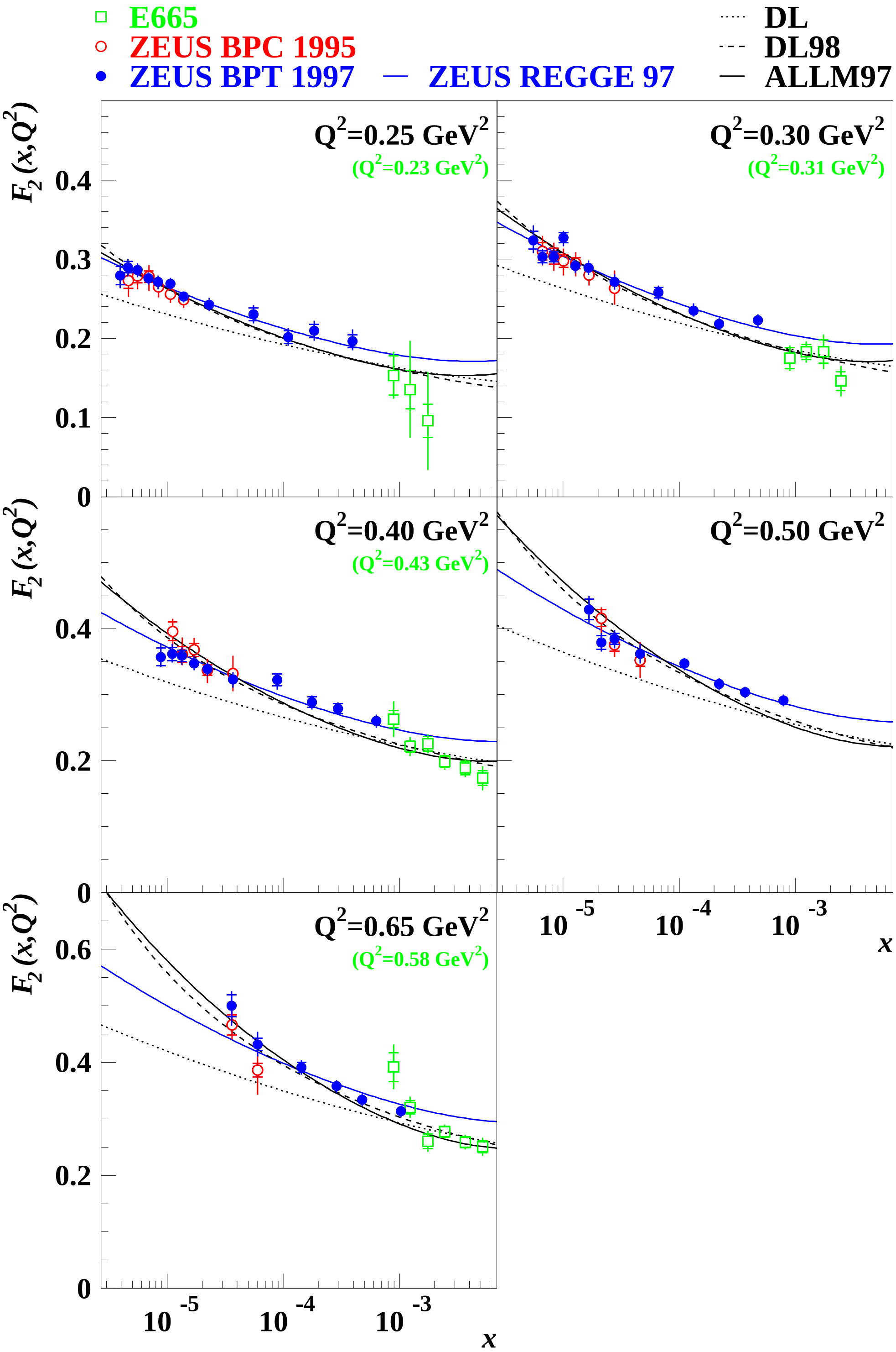

Regge inspired parameterisations:
(DL98, ALLM97, ZEUSRegge)
provide a good description of the transition region

Extrapolation to Photoproduction

$$\boxed{\sigma_{tot}^{\gamma^* p} = 4\pi^2\alpha/Q^2 \cdot F_2}$$

ZEUS 1997 Preliminary

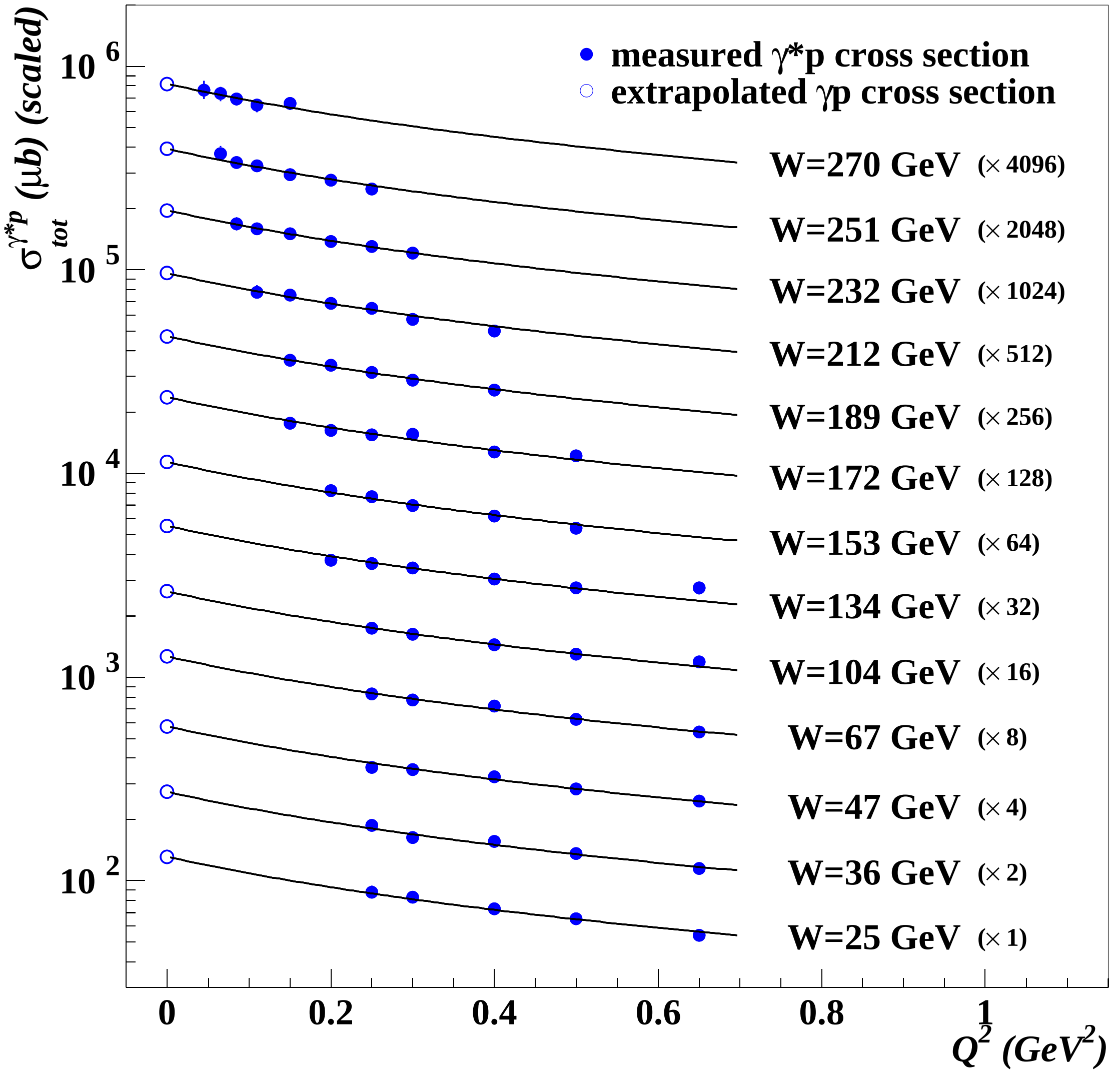

By assuming Q^2 dependence of $\sigma_{tot}^{\gamma^* p}$ of GVDM:

$$\boxed{\sigma_{tot}^{\gamma^* p}(W^2, Q^2) = \frac{m_0^2}{m_0^2 + Q^2}\,\sigma_{tot}^{\gamma p}(W^2)}$$

can extrapolate data to compare with photoproduction ($Q^2 \sim 0$) cross-section $\sigma_{tot}^{\gamma p}$:

Extrapolation to Photoproduction

ZEUS 1997 (Preliminary)

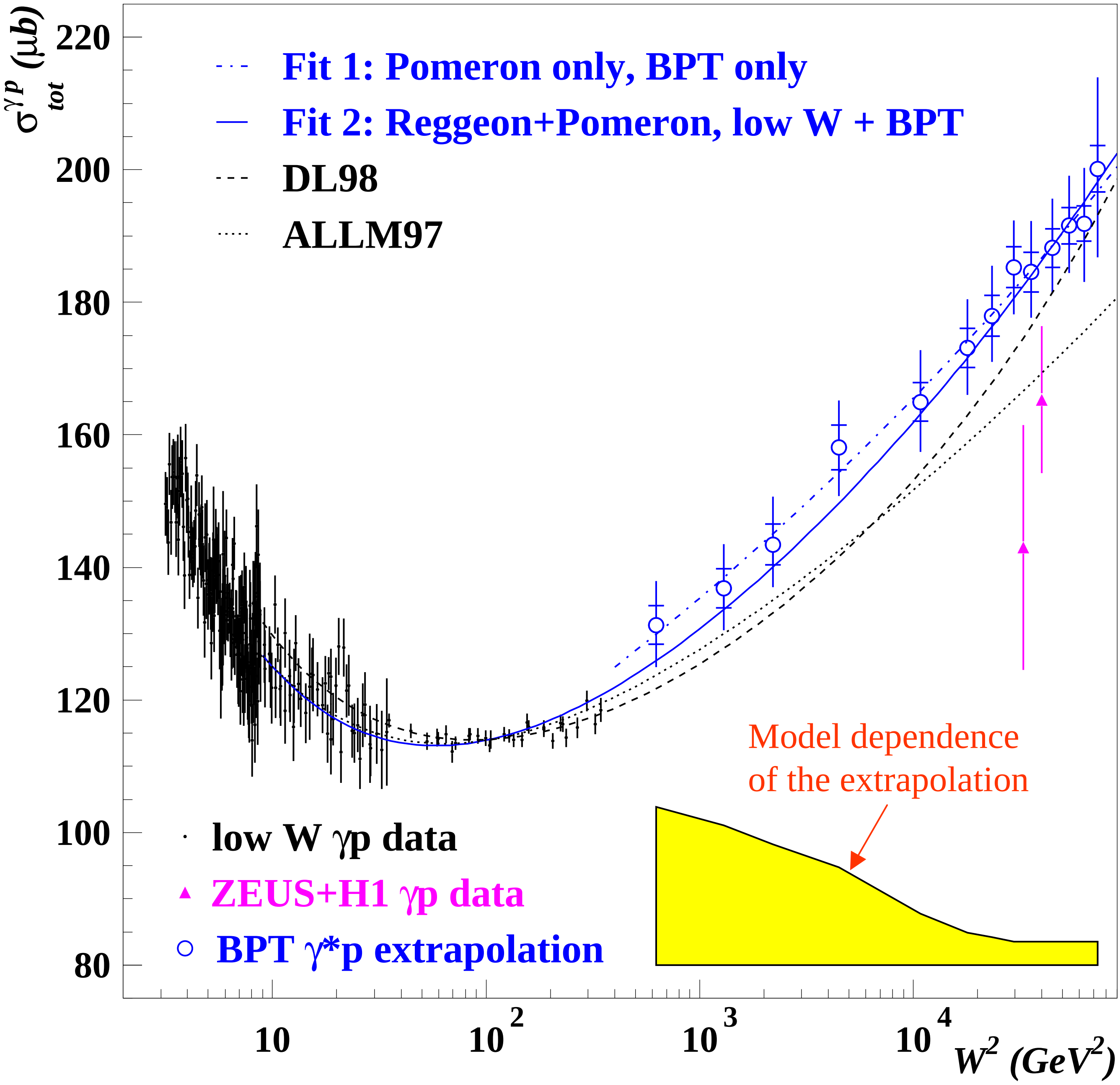

W^2 dependence of $\sigma_{tot}^{\gamma p}$ à la Regge:

$$\sigma_{tot}^{\gamma p}(W^2) = A_{\mathbb{R}} W^{2(\alpha_{\mathbb{R}}(0)-1)} + A_{\mathbb{P}} W^{2(\alpha_{\mathbb{P}}(0)-1)}$$

Results ($\alpha_{\mathbb{R}}(0) = 0.5$, $A_{\mathbb{R}}$, $A_{\mathbb{P}}$, $\alpha_{\mathbb{P}}(0)$ free parameters):

"Fit 2": **$\alpha_{\mathbb{P}}(0) = 1.105 \pm 0.001(\mathrm{stat}) \pm 0.007(\mathrm{syst})$**

consistent with Cudell at al. fit: $1.096^{+0.012}_{-0.010}$

F_2 at Medium Q^2: Precision Data

Recent data made measurement of F_2 possible with improved precision due to higher event statistics and the new backward silicon tracker in H1:

- typical errors ~ 1% (stat) and ~ 2-3% (syst)
  $\Rightarrow$ approaching fixed target experiments!
- Syst. error dominant up to $Q^2 \approx 1000$ GeV^2

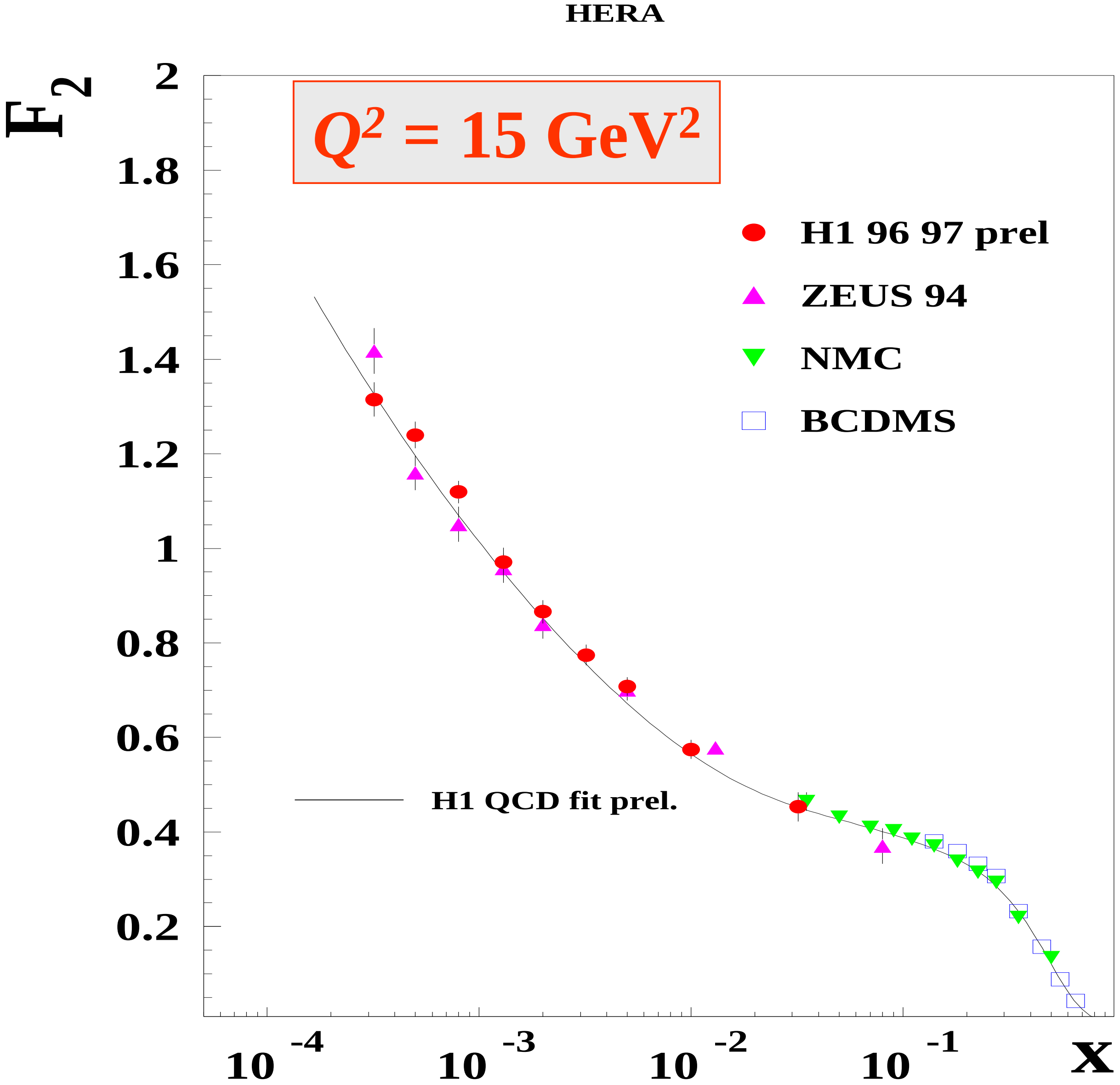

- **Strong rise of F_2 at HERA regime**
  ($q(x) \propto F_2/x$ $\Rightarrow$ quark density is zooming up)
- **Good agreement between H1 and ZEUS**

Overview of F_2 Measurements

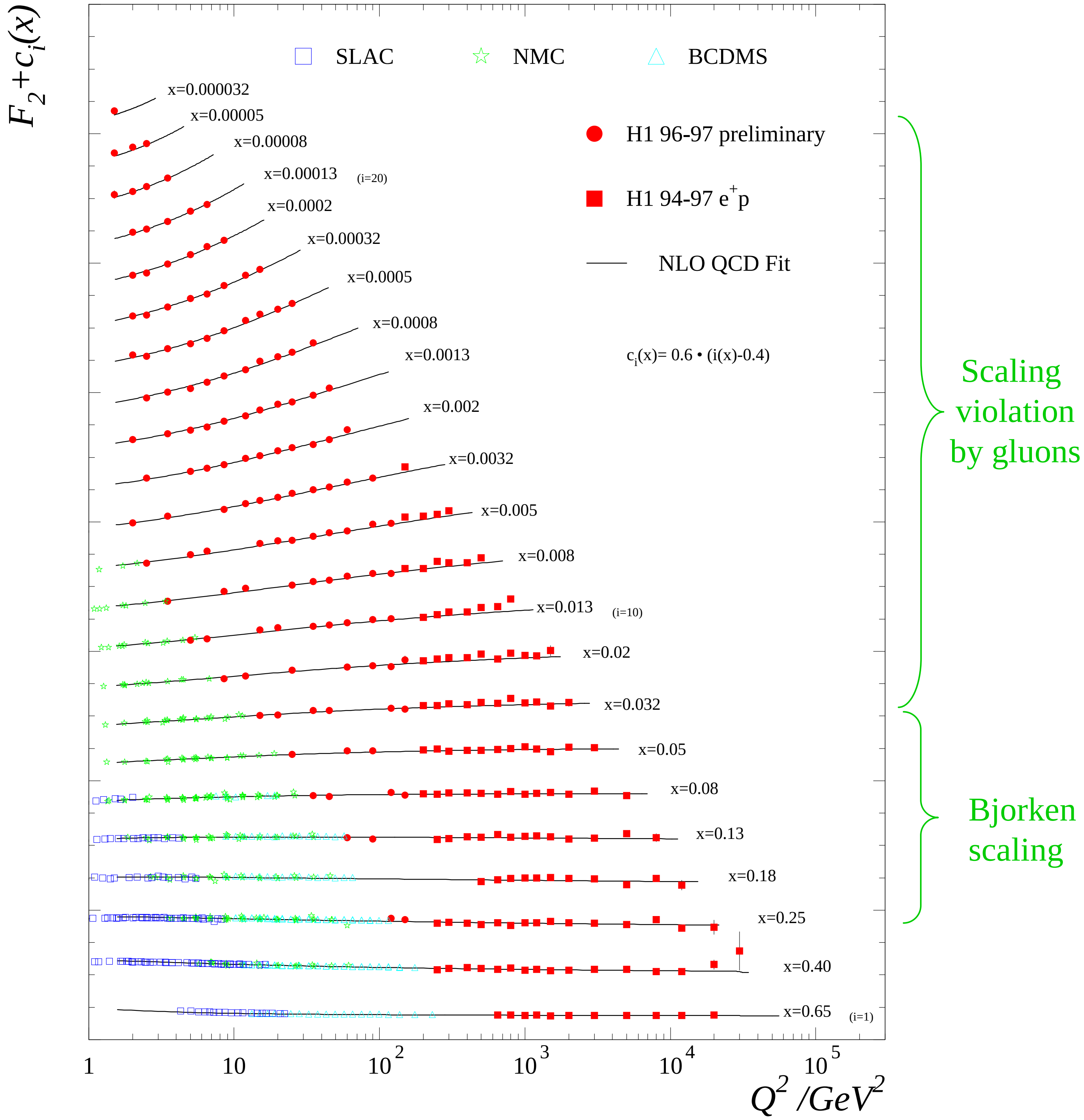

- NLO DGLAP fit gives good description of the HERA and fixed target data
- Scaling violations well interpreted by QCD

⇒ No indication of $(\ln 1/x)^n$ corrections in the HERA regime

Comparison with Fixed Target

Long standing controversy between μp (NMC, E665) and νN (CCFR) data:

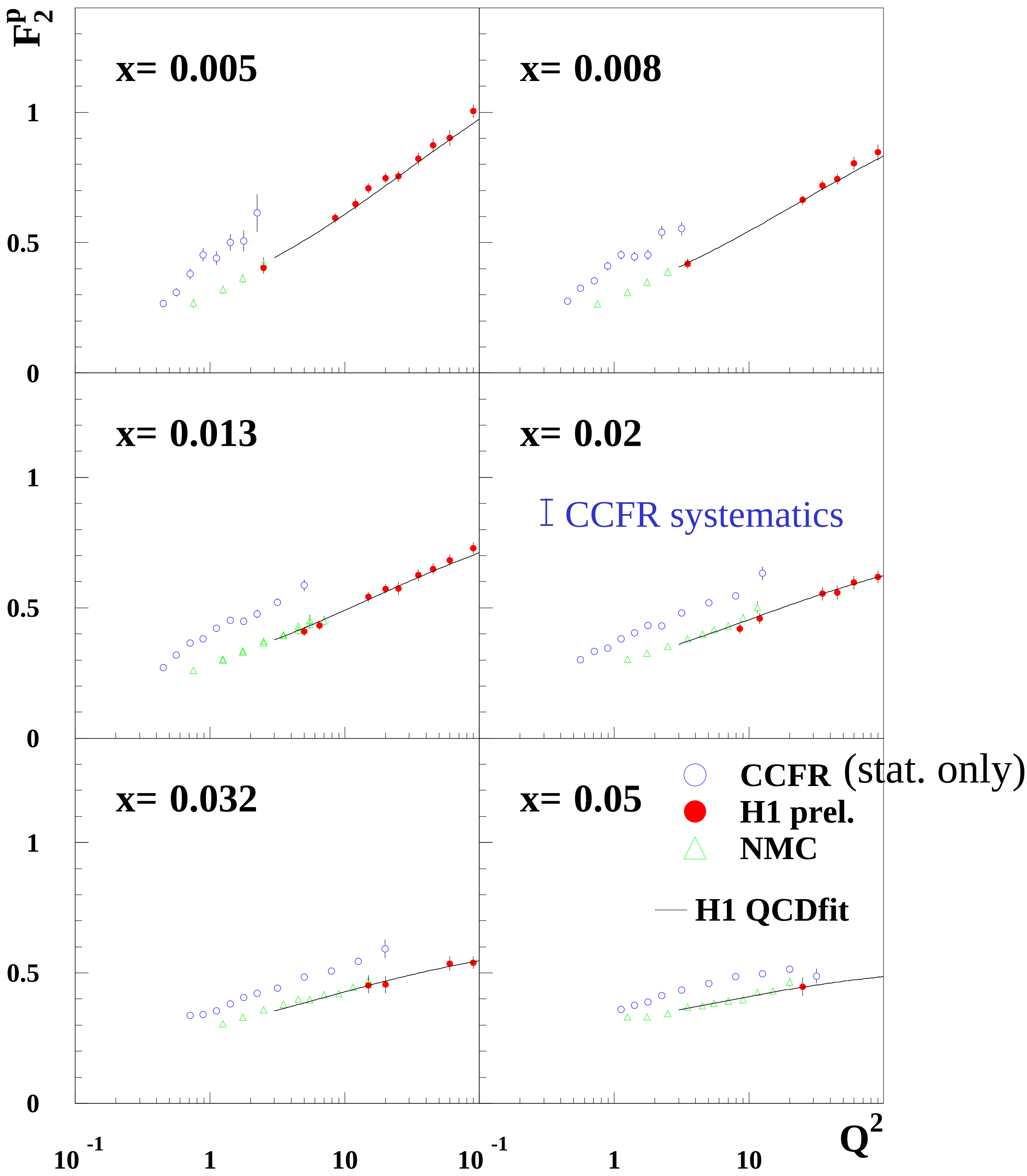

H1 data overlap and extrapolate well to μp data

CCFR data being re-analysed, with new treatment of charm and shadowing

Derivatives of F_2

The slopes $\dfrac{d\ln F_2}{d\ln \frac{1}{x}}$ and $\dfrac{dF_2}{d\ln Q^2}$ contain a lot of information:

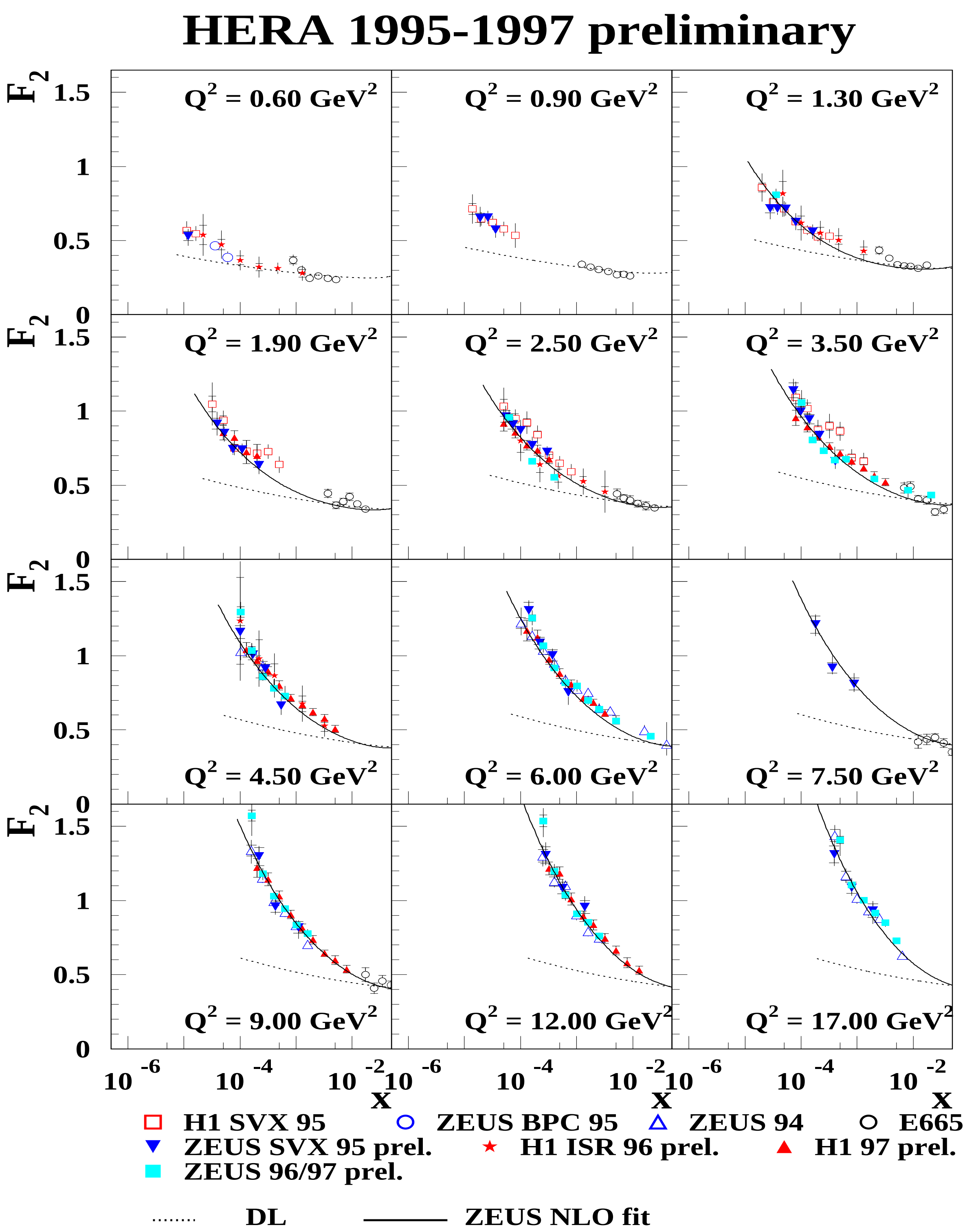

The x-slope is small at small Q^2, then increases.

Fit: $F_2 = \mathrm{const} \cdot x^{-\lambda_{\mathrm{eff}}}$ at small x (giving: $d\ln F_2/d\ln(1/x) = \lambda_{\mathrm{eff}}$)

Fit to $F_2 \propto x^{-\lambda_{\text{eff}}}$ vs. Q^2 at small x

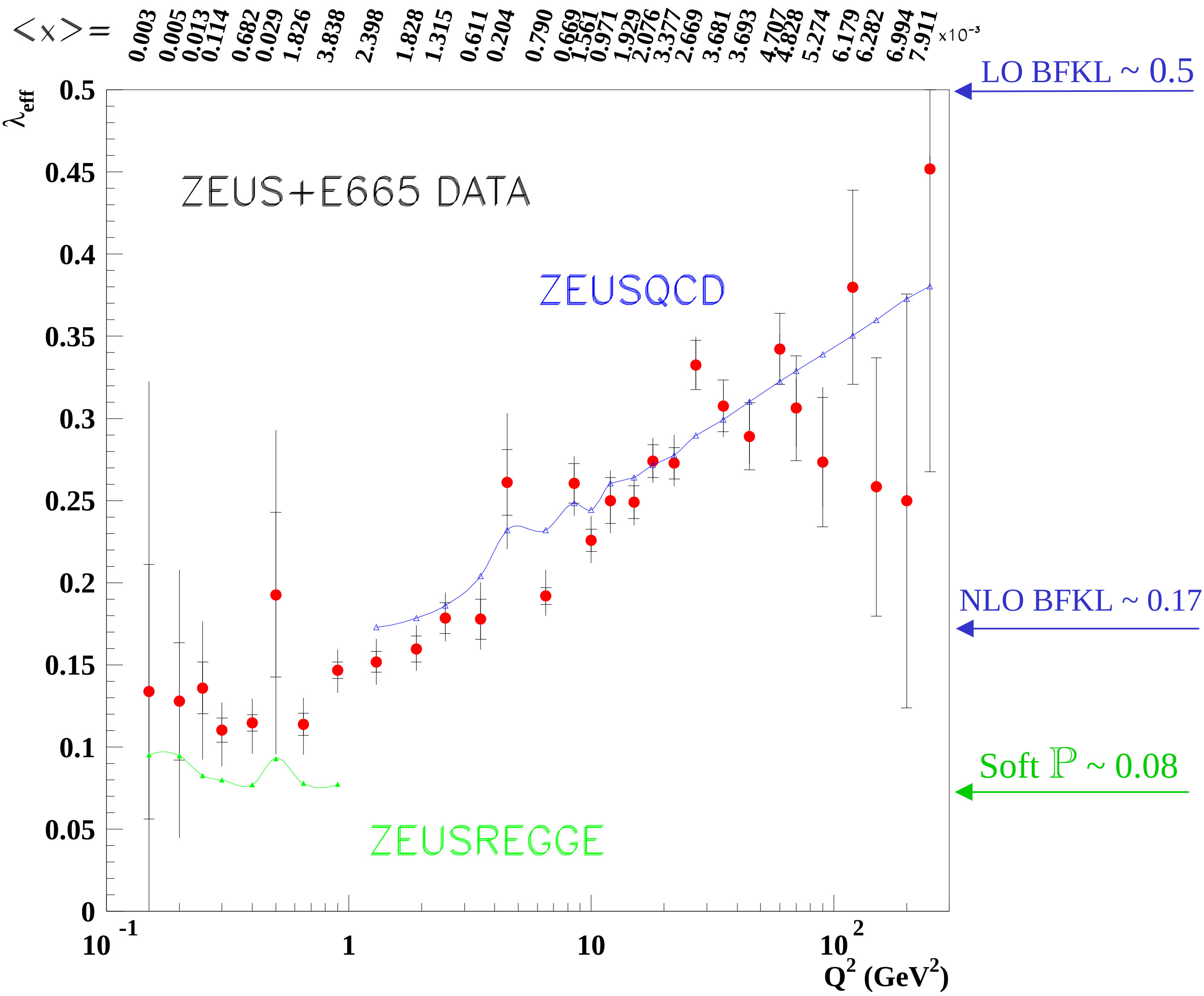

Since: $1/x \sim W^2 \Rightarrow x^{-\lambda_{\text{eff}}} \sim W^{2\lambda_{\text{eff}}}$

$\Rightarrow s^{2(\alpha_{\mathbb{P}}(0)-1)}$ Regge dependence of cross sections

$\Rightarrow$ the x-exponent λ_{eff} corresponds to the Regge $\varepsilon = \alpha_{\mathbb{P}}(0) - 1$

Notice: λ_{eff} different in Regge and LO (NLO) BFKL approaches

- Smooth rise of the slope parameter λ_{eff}
- In agreement with Regge expectations at low Q^2
- Described by pQCD NLO fit using DGLAP evolution
- As for F_2, no need for $(\ln 1/x)^n$ BFKL terms.

$dF_2(x,Q^2)/d\ln Q^2$

DGLAP evolution equation: $$\frac{dF_2}{d\ln Q^2} = \frac{\alpha_s}{2\pi}\int_x^1 \frac{dz}{z}\left[F_2 \cdot P_{qq} + g \cdot P_{qg}\right]$$

Logarithmic slope $dF_2/d\ln Q^2$ derived from data fitting: $F_2 = a + b \cdot \ln Q^2$ at fixed x

The turn over at small x

(a kinematic effect due to the average over a Q^2 range)

reflects a smaller rise of the derivatives, i.e. the gluon density, for $x \to 0$ when Q^2 decreases below few GeV^2

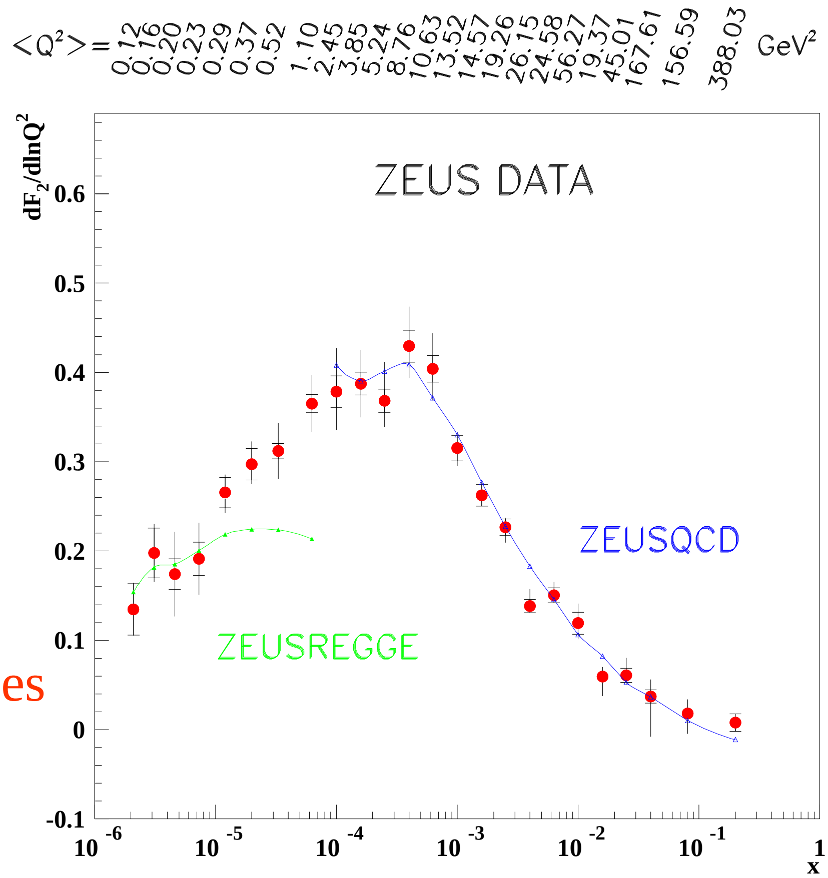

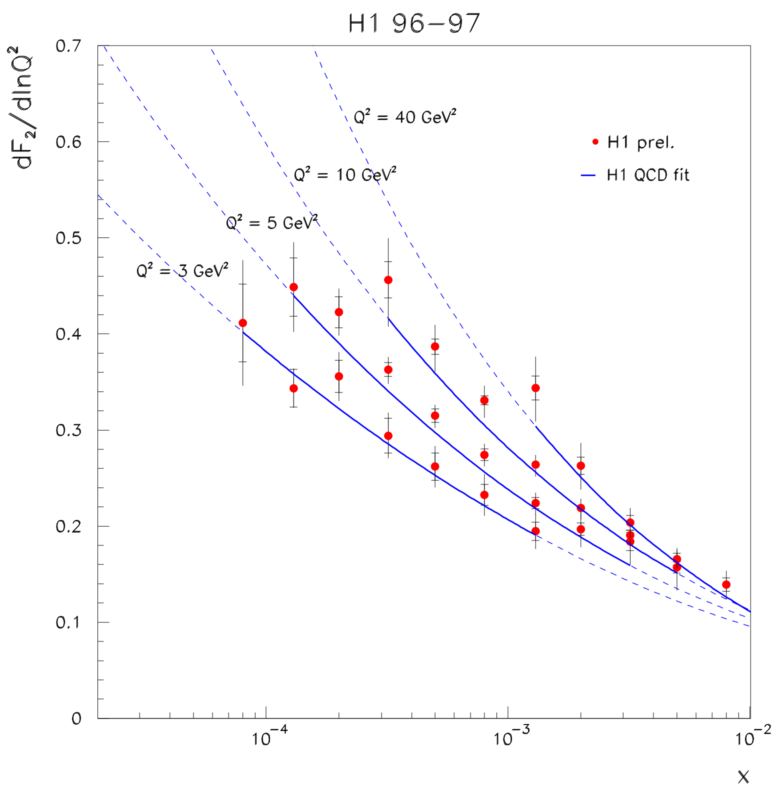

Notice: the slopes taken at fixed Q^2 are monotonically increasing, as expected in pQCD

NLO pQCD Fit to F_2

H1 DGLAP NLO fit:

- H1 and NMC data used, $\overline{\text{MS}}$ renormalisation scheme, $3.5 < Q^2 < 3000$ GeV^2, as($M_Z{}^2$) = 0.118
- three light flavours; c,b from Boson Gluon Fusion
- Apply momentum sum rule

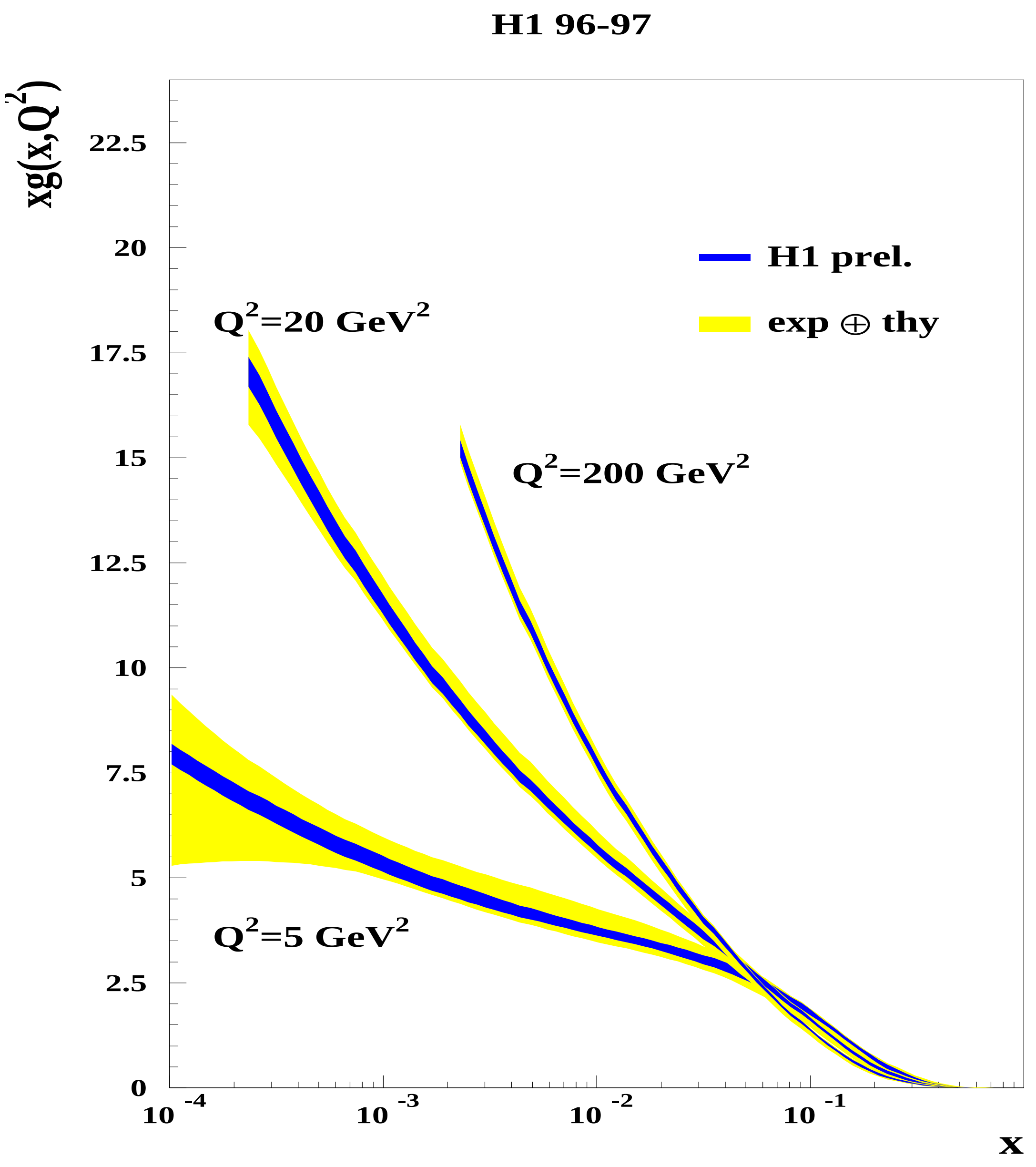

- Inner error bands: exp. Uncertainties, few percent at low *x*
- Outer error bands: uncertainties depending on
  - fit parameters ($Q_{min}{}^2$, $Q_0{}^2$, α_s, m_c)
  - choice of parameterisation for initial distributions.

NLO pQCD Fit to F_2

ZEUS DGLAP NLO fit:

- Gluon (xg), Sea quark (xS) and u - d difference ($x\Delta_{ud}$) parameterised as: $A \cdot x^{\delta} \cdot (1-x)^{\eta} \cdot$ polynomial in $\sqrt{x}$
- Input u,d valence distributions from MRS(R2)
- Apply momentum sum rule

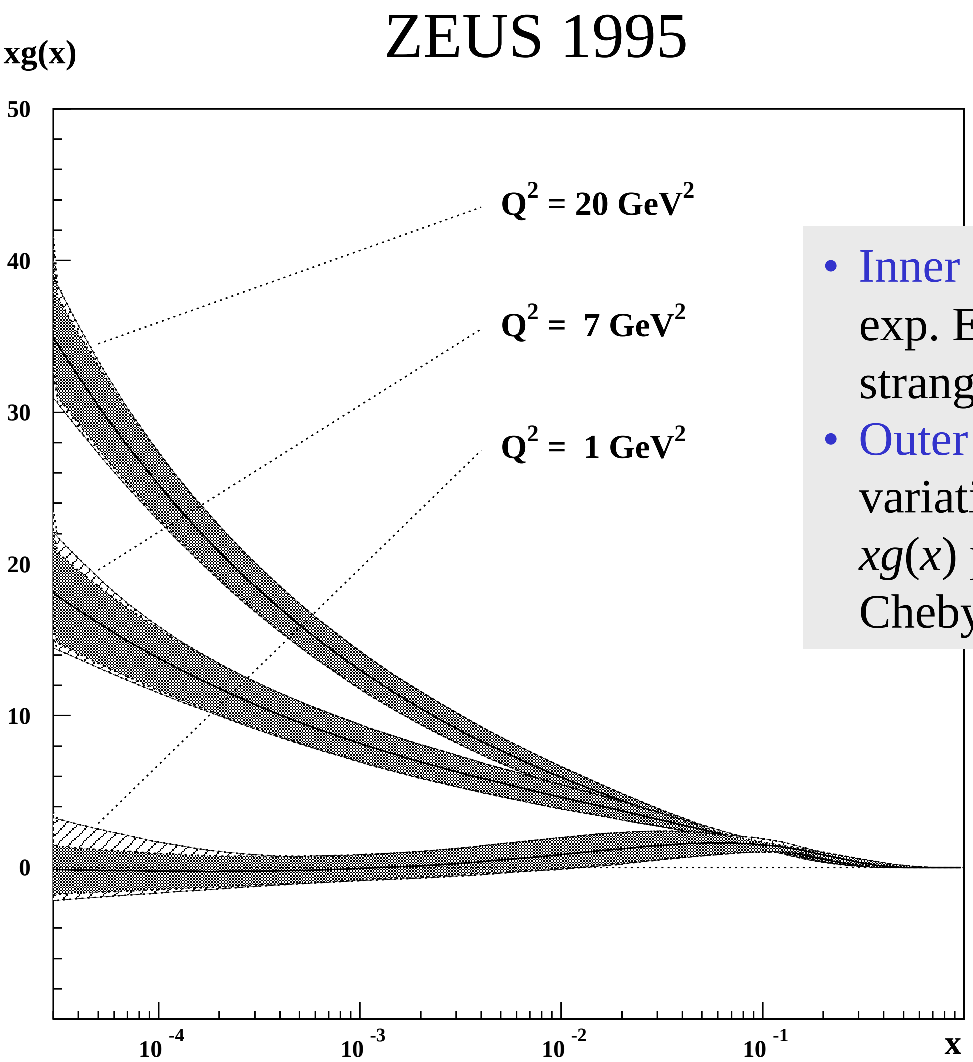

- Inner error bands: exp. Errors on α_s, m_c and strange quark content ΔK_s
- Outer error bands: variation of Q_0^2 and $xg(x)$ parameterised with Chebycheff polynomials.

Strong rise of gluon density at large Q^2 but consistent with zero at $Q^2 = 1\ GeV^2$

QCD Fit to F_2: Gluon and Singlet

Quark singlet distribution : $x\Sigma = \sum_{i=u,d,s} (xq_i + x\bar{q}_i)$

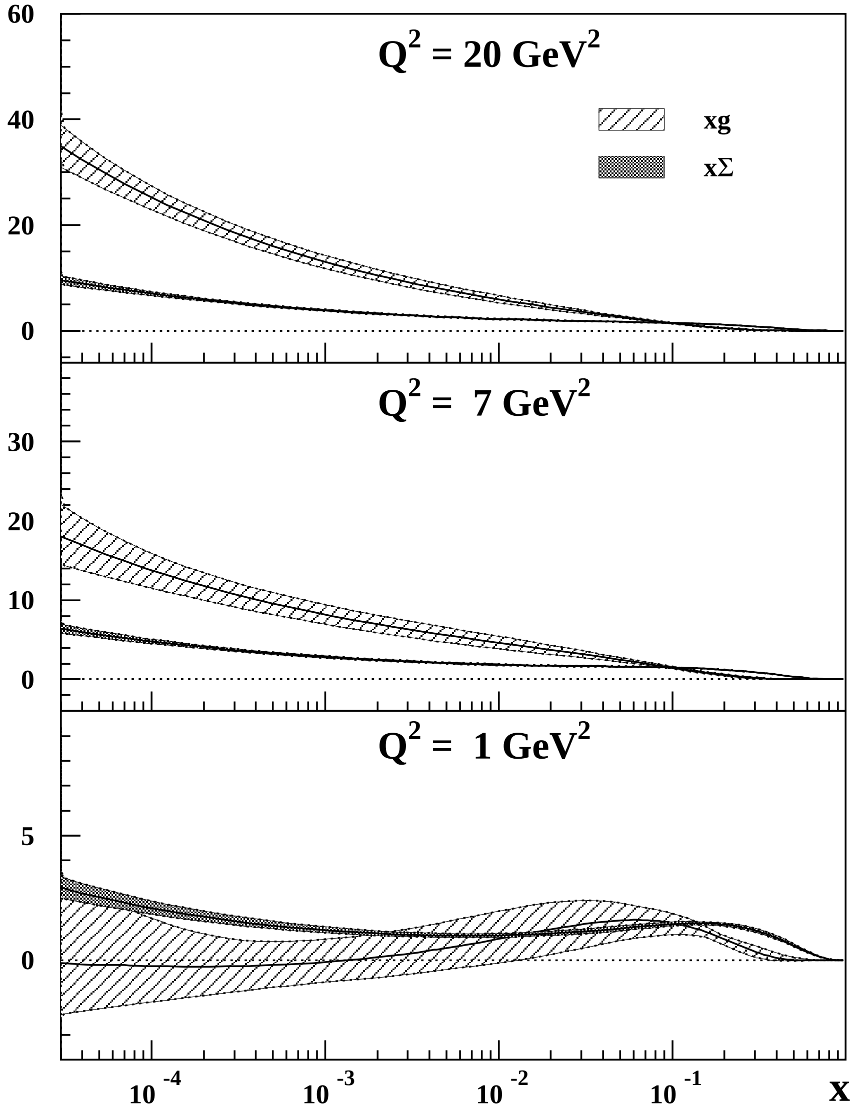

- At Q^2 = 1 GeV^2, Sea is still rising but Gluon at small x is compatible with zero
- Uncertainty for gluon at lowest x,Q^2 is large

Although error band goes negative (possible in NLO backward evolution):

- F_L and F_2^{charm} stay positive
- the fit can be extended down to Q^2 = 0.4 GeV^2 without deteriorating its quality

$\Rightarrow$ NLO DGLAP does not break down before the formalism becomes suspect

Extraction of F_L

DIS cross section:
(for $Q^2 \ll M_Z^2$ and neglecting radiative corrections)

$$\frac{d^2\sigma^{ep}_{NC}}{dxdQ^2} = \frac{2\pi\alpha^2}{xQ^4} \cdot \left[\left(1+(1-y)^2\right)F_2\left(x,Q^2\right) - y^2 F_L\left(x,Q^2\right)\right]$$

Remember: F_L relevant only at high y.

Let's define the reduced cross section σ_r as:

$$\frac{d^2\sigma^{ep}_{NC}}{dxdQ^2} = \frac{2\pi\alpha^2}{xQ^4} \cdot (1+(1-y)^2) \cdot \sigma_r$$

$$\text{where: } \sigma_r = F_2 - \frac{y^2}{1+(1-y)^2} \cdot F_L$$

$$\Rightarrow \sigma_r = F_2 - F_L \quad \text{at large } y$$

H1 uses the "Subtraction method":
indirect access to F_L from large y cross sections using assumption on F_2 by extrapolation of DGLAP fit from low y

$$\Rightarrow \mathrm{F_L} \approx \mathrm{F_2} - \sigma_\mathrm{r} \quad \text{at large } y$$

Extraction of F_L

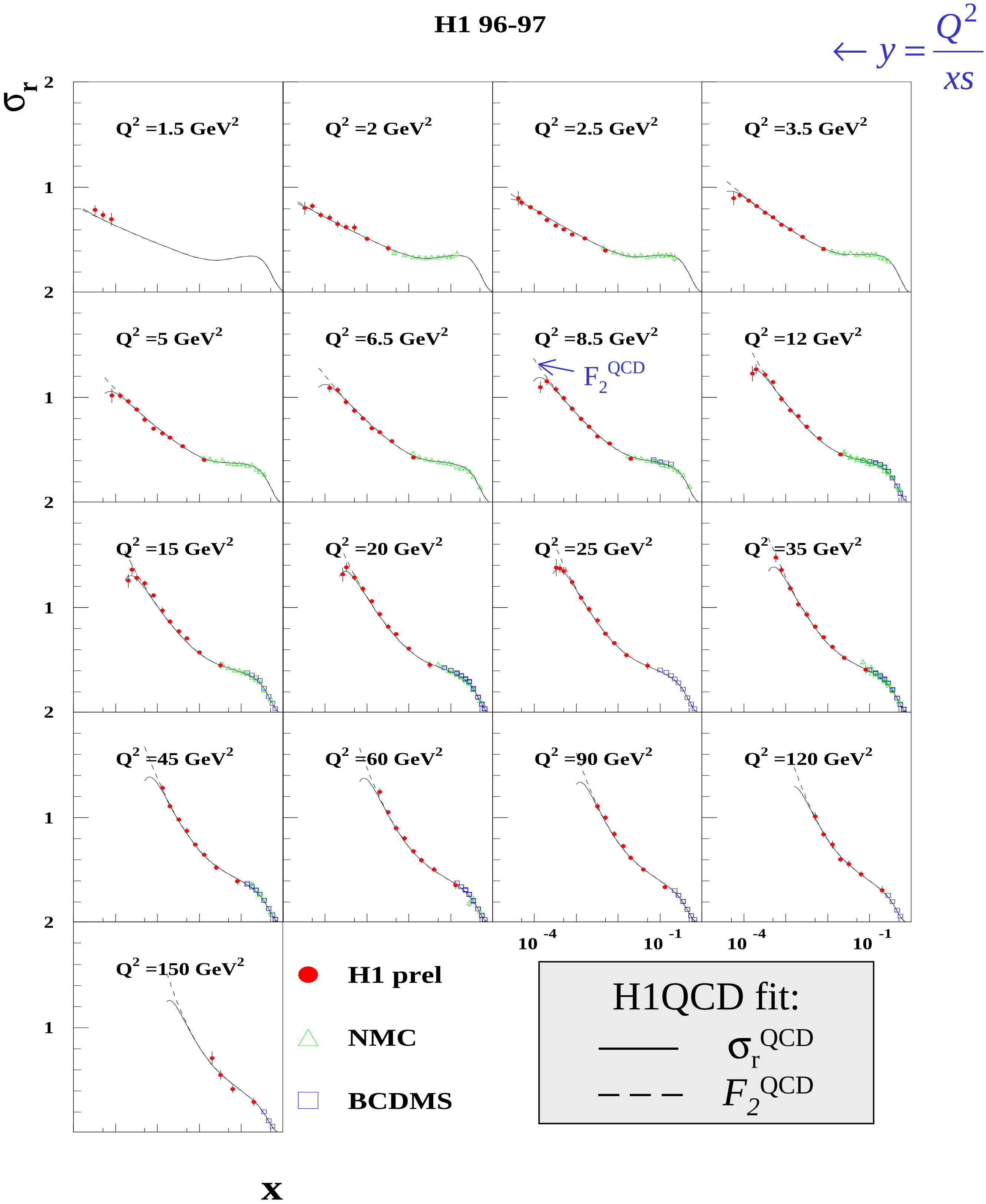

- F_2^{QCD} is the H1 QCD NLO fit for y < 0.35
- Extrapolate F_2^{QCD} results to high *y*
- $F_L \sim F_2^{QCD} - \sigma_r$ at high *y*

Extraction of F_L

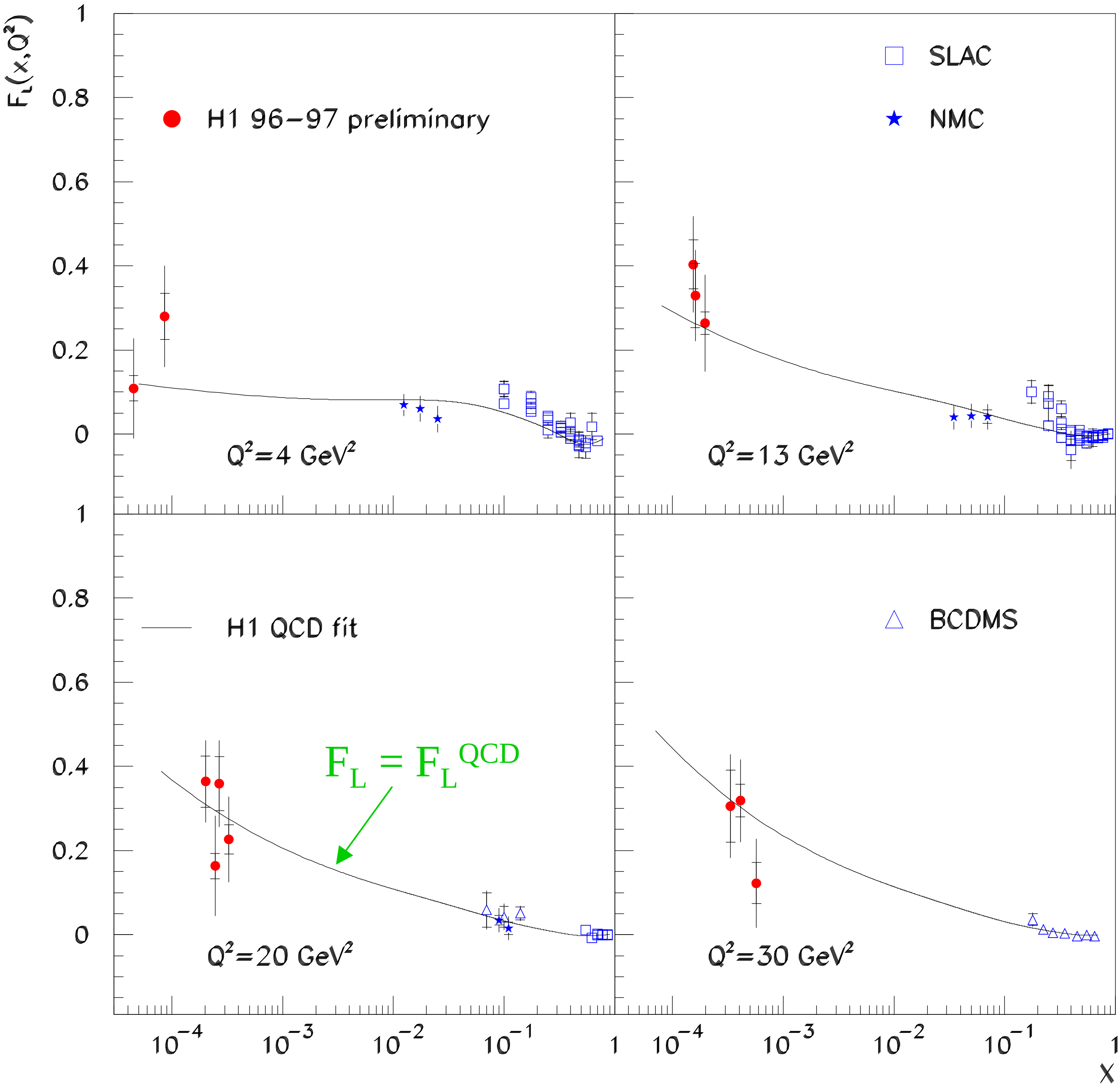

Extracted F_L well described by F_L^{QCD} from H1 NLO QCD fit:

$$F_L^{QCD} = \frac{\alpha_s}{4\pi} x^2 \int \frac{dz}{z^3} \left[\frac{16}{3} F_2 + 8 \sum e_i^2 \left(1 - \frac{x}{z} \right) zg \right]$$

i.e., using only F_2 data, derive gluon and parton distributions by scale violations and then calculate F_L^{QCD}

Rise towards low x consistent with $xg(x)$ behaviour:

F_2^{charm} from D* mesons in DIS

Charm cross section in DIS is expected to be dominated by **Boson-Gluon-Fusion**
i.e. by gluon density

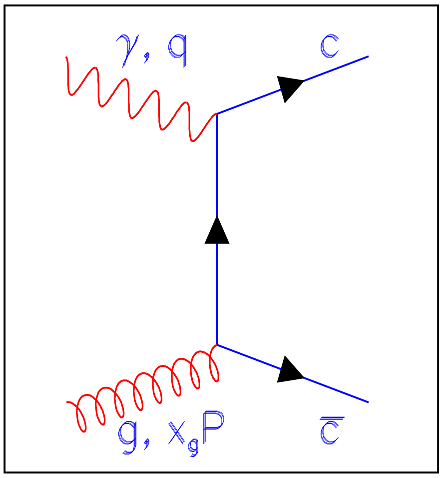

- Measure visible cross section for D*
- extrapolate outside kinematic region in p_T,η
- extract F_2^{charm}:

Very effective test of QCD:

F_2^{charm} calculable from pQCD knowing $xg(x)$

$$F_2 \Rightarrow xg(x) \Rightarrow \sigma^{C\bar{C}} \equiv xg(x) \otimes \mathrm{BGF} \Rightarrow F_2^{charm}$$

$$F_2^{charm} \Leftarrow \sigma^{C\bar{C}} \Leftarrow \text{extrap.}\,\eta, p_\perp \Leftarrow \text{measure } D^*$$

Direct measurement of F_2^{charm}

F_2^{charm} from D* mesons in DIS

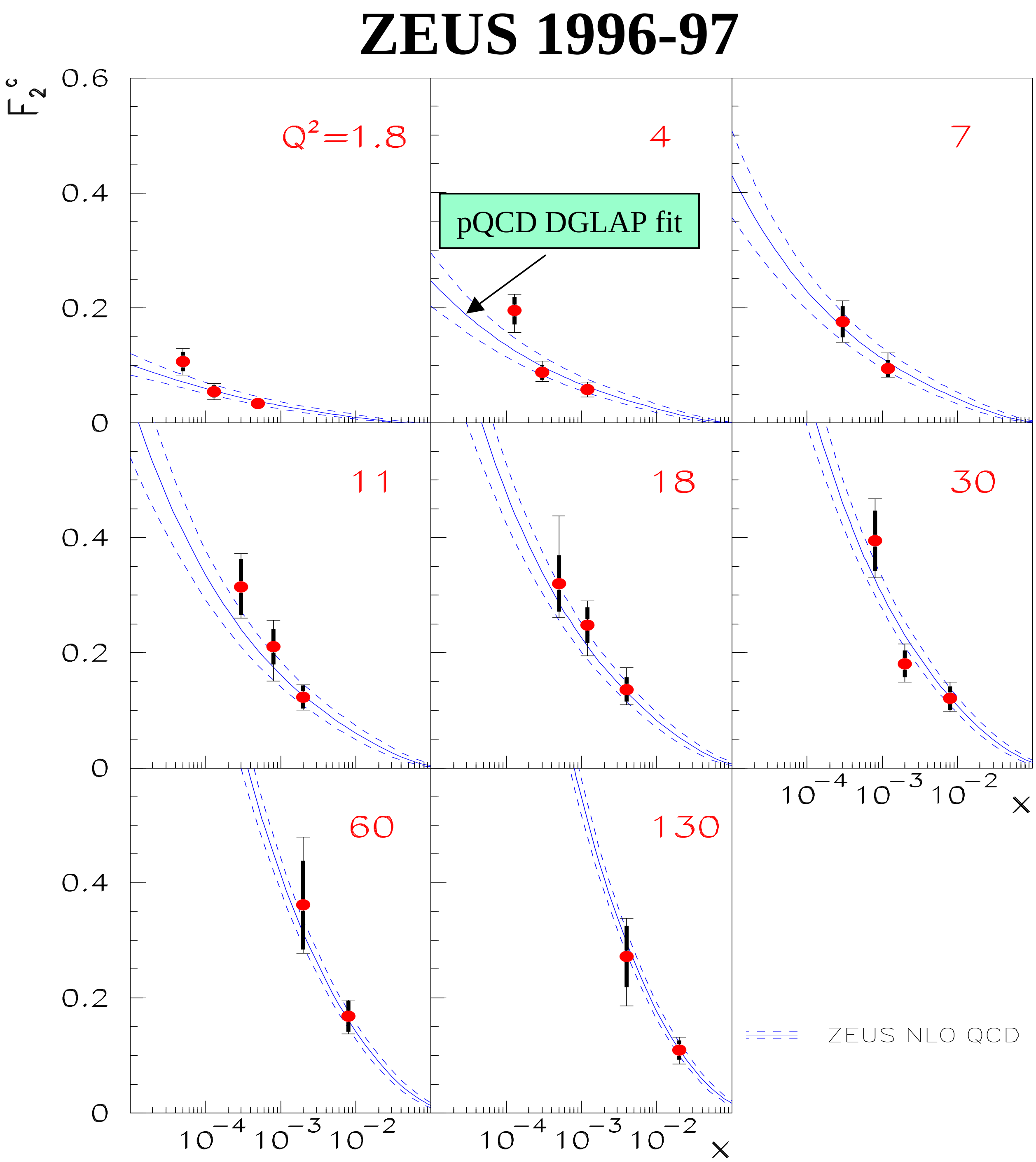

- Steep rise of F_2^{charm} as we go to smaller x
- agreement with ZEUS NLO QCD fit: indication that BGF is the dominant mechanism for charm production at HERA

F_2^{charm}/F_2 vs. x in Q^2 bins

ZEUS 1996-97

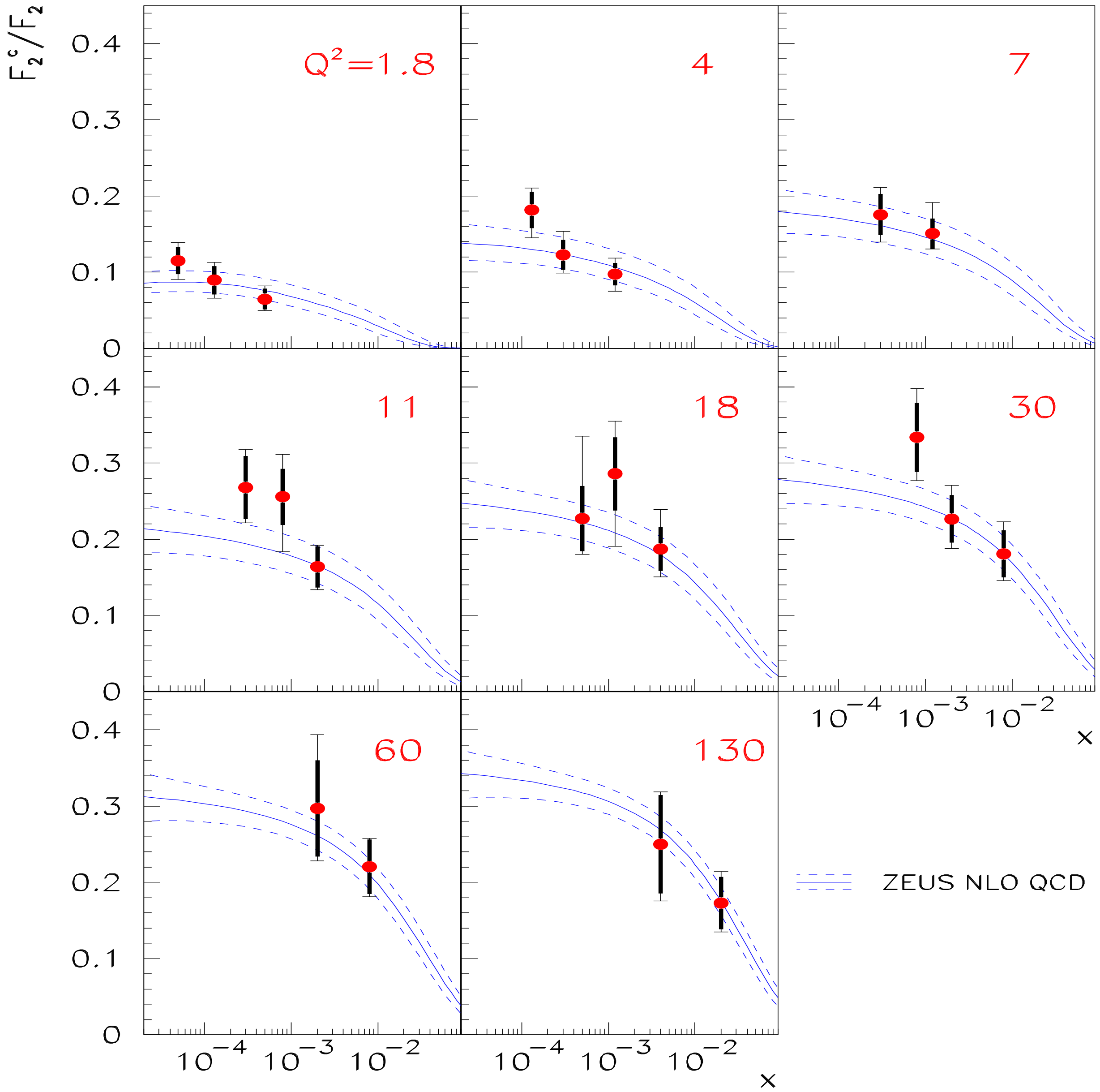

- F_2^{charm} rises more rapidly than F_2
  $\Rightarrow$ F_2^{charm} dominated by gluon contribution, while F_2 has also sea quarks
- F_2^{charm} is 25% of F_2 at low x and high Q^2, but "only" 10% at $Q^2 = 1.8$ GeV^2,
  $\Rightarrow$ ratio glue/(glue+sea) decreasing for $Q^2 \rightarrow 0$

High Q^2 Neutral Currents

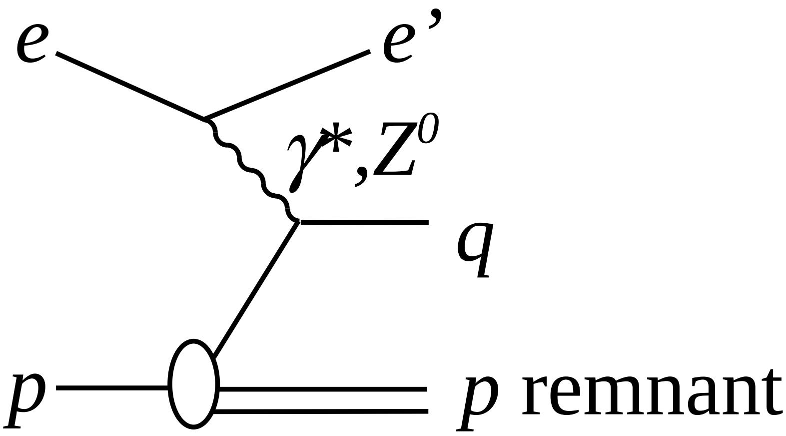

$$\frac{d^2\sigma_{NC}^{e^\pm p}}{dxdQ^2} = \frac{2\pi\alpha^2}{xQ^4}\cdot\left[Y_+\tilde{F}_2(x,Q^2) \mp Y_- x\tilde{F}_3(x,Q^2)\right]$$

where:

$$Y_\pm = 1 \pm (1-y)^2$$

$$\tilde{F}_2 = F_2^{em} + \frac{Q^2}{Q^2+M_Z^2}F_2^{\gamma Z} + \left(\frac{Q^2}{Q^2+M_Z^2}\right)^2 F_2^Z$$

$$\tilde{F}_3 = \frac{Q^2}{Q^2+M_Z^2}F_3^{\gamma Z} + \left(\frac{Q^2}{Q^2+M_Z^2}\right)^2 F_3^Z$$

Handle on xF_3 given by the $\mp$ sign due to the different charge of the lepton beam.
Data with e$^-$ beams to access xF_3:
γZ interference already seen

High Q^2 Neutral Currents: $d\sigma^{e^+p}/dQ^2$

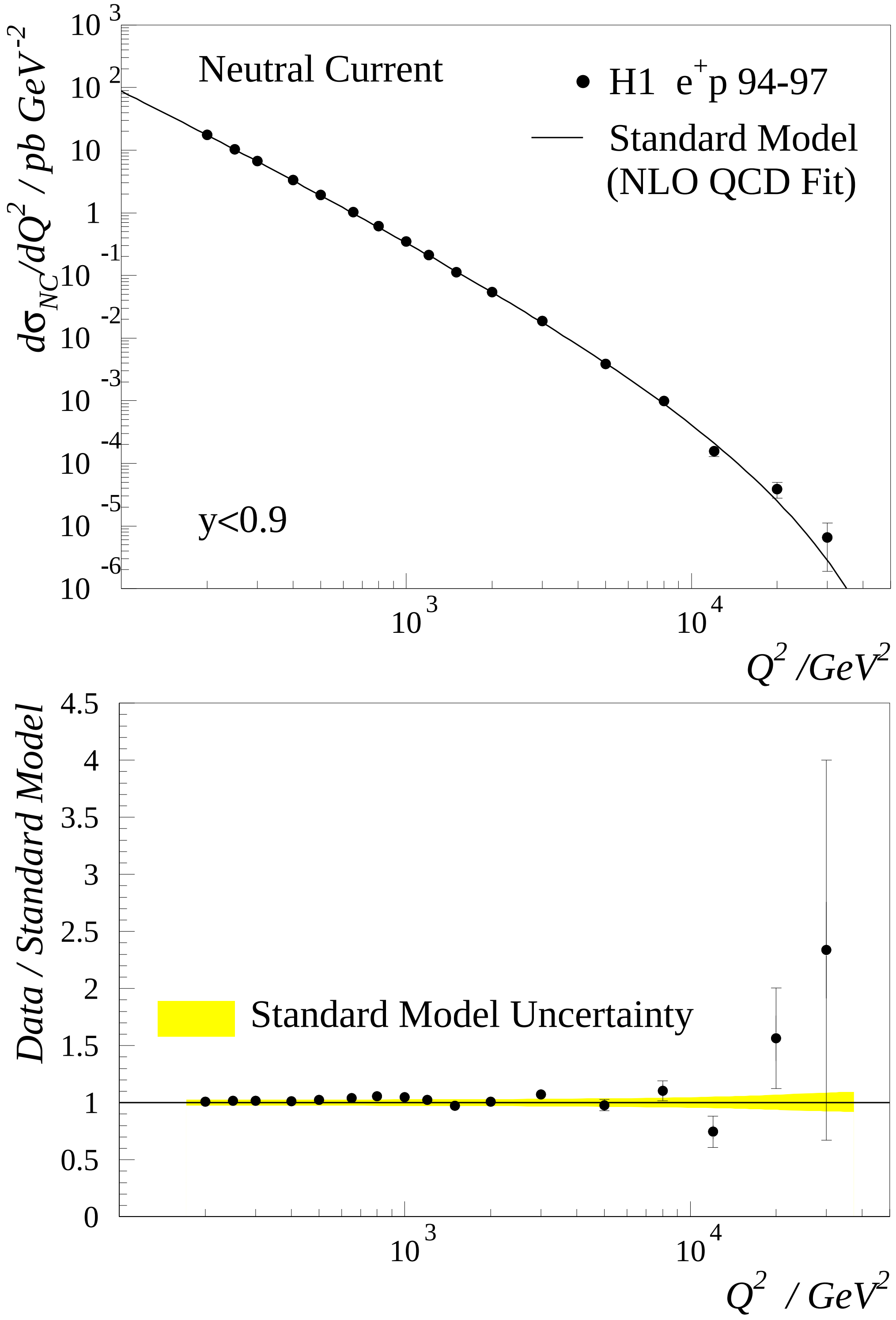

- $d\sigma^{e^+p}/dQ^2$ falls over 7 orders of magnitude
- NLO QCD fit to low Q^2 data ($Q^2 < 120$ GeV^2) works well for high Q^2
- Benchmark for the Standard Model
- Larger luminosity needed to constrain PDFs

High Q^2 Neutral Currents: e^+ vs. e^-

$$\frac{d^2\sigma_{NC}^{e^\pm p}}{dx dQ^2} = \frac{2\pi\alpha^2}{xQ^4}\cdot \underbrace{\left[Y_+\tilde{F}_2\left(x,Q^2\right)\mp Y_- x\tilde{F}_3\left(x,Q^2\right)\right]}_{\tilde{\sigma}_{NC}}$$

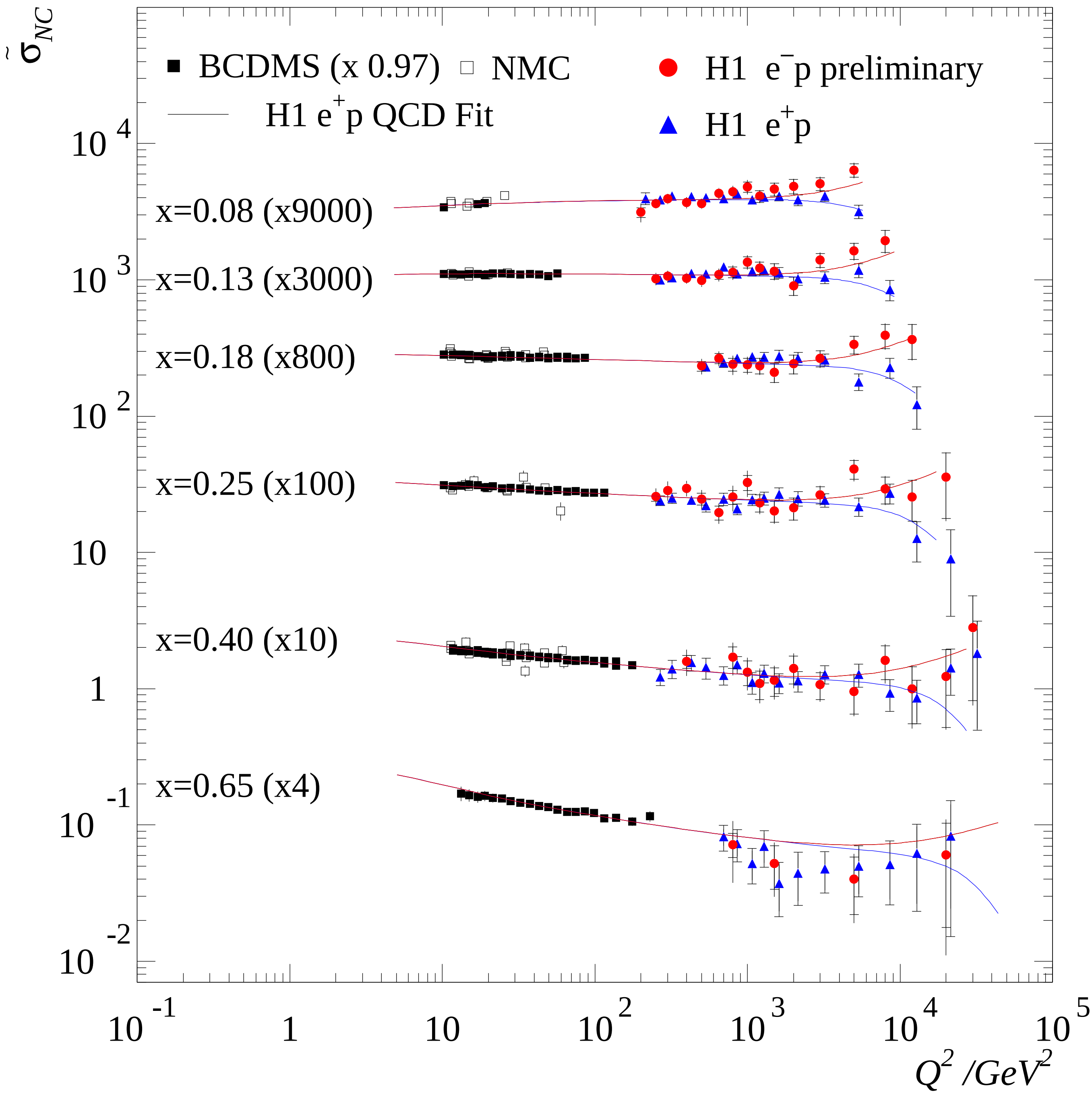

For $Q^2 > 3000$ GeV^2, e^-p measurements are above e^+p, in agreement with SM γZ interference

High Q^2 Charged Currents

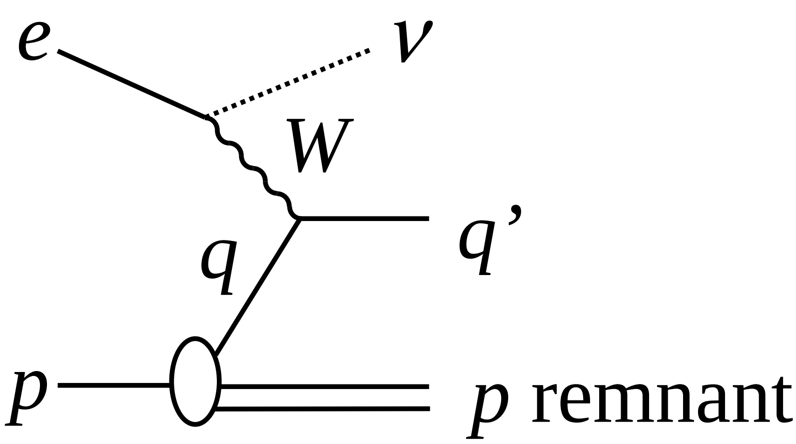

$$\frac{d^2\sigma_{CC}^{e^{\pm}p}}{dx\,dQ^2} = \frac{G_F^2}{2\pi x} \cdot \left[\frac{M_W^2}{Q^2 + M_W^2}\right]^2 \cdot \Phi_{CC}^{\pm}(x, Q^2)$$

where, in the naive quark parton model:

$$\Phi_{CC}^{+}(x, Q^2) = \bar{u} + (1-y)^2 \cdot (d + s)$$

$$\Phi_{CC}^{-}(x, Q^2) = u + (1-y)^2 \cdot (\bar{d} + \bar{s})$$

At large x and Q^2:

– Probe valence u,d quarks

– $\sigma_{\mathrm{CC}}^{e^-p} > \sigma_{\mathrm{CC}}^{e^+p}$, since in the case of e^-:
directly sensitive to quarks,
helicity factor $(1-y)^2$ multiplies antiquark density

High Q^2 Charged Currents: $d\sigma^{e^+p}/dx$

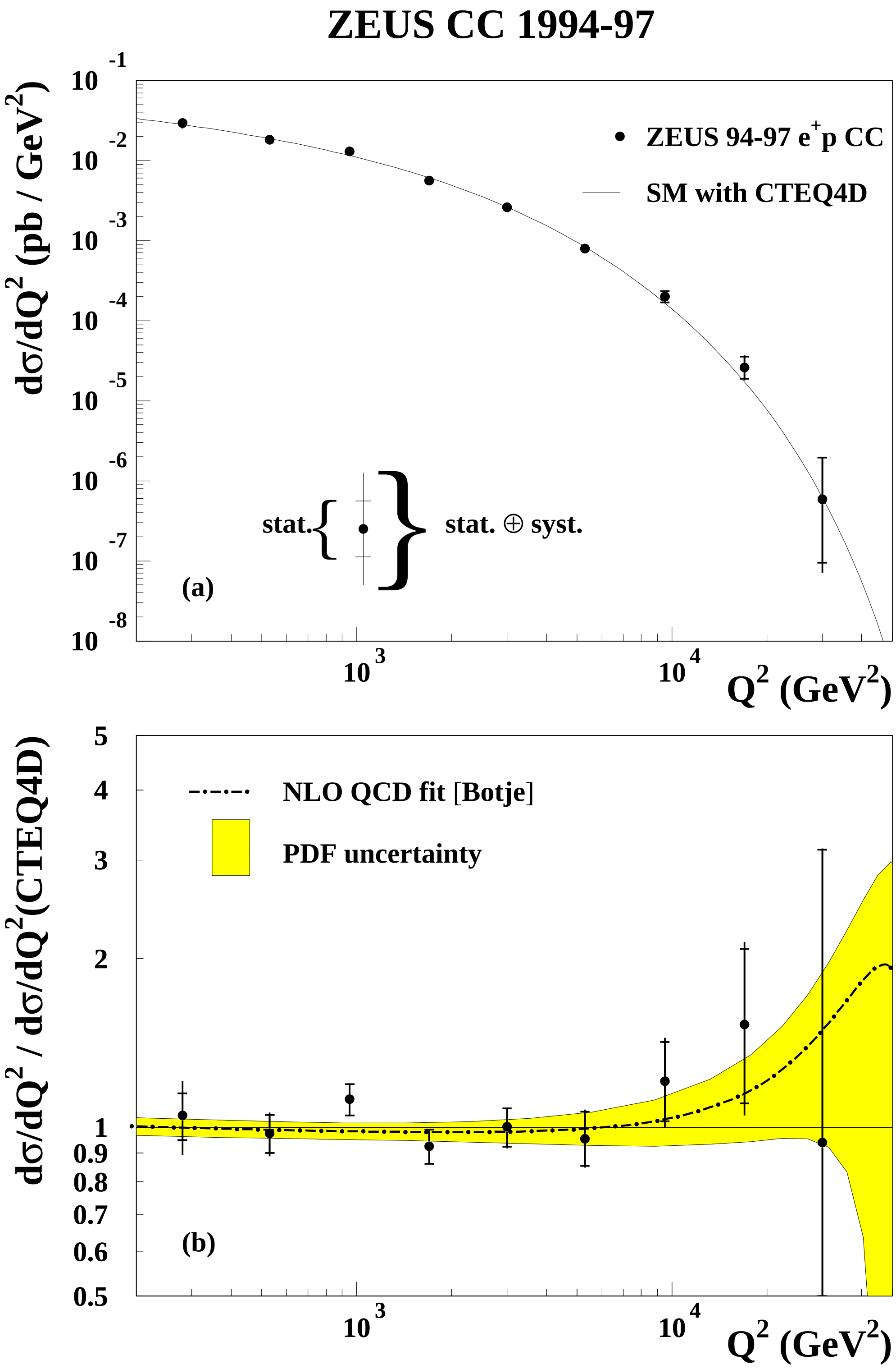

- Reasonable agreement between SM and data
- At high Q^2, data above CTEQ4 -
  well described by NLO pQCD fit

High Q^2 Charged Currents: e^+ vs. e^-

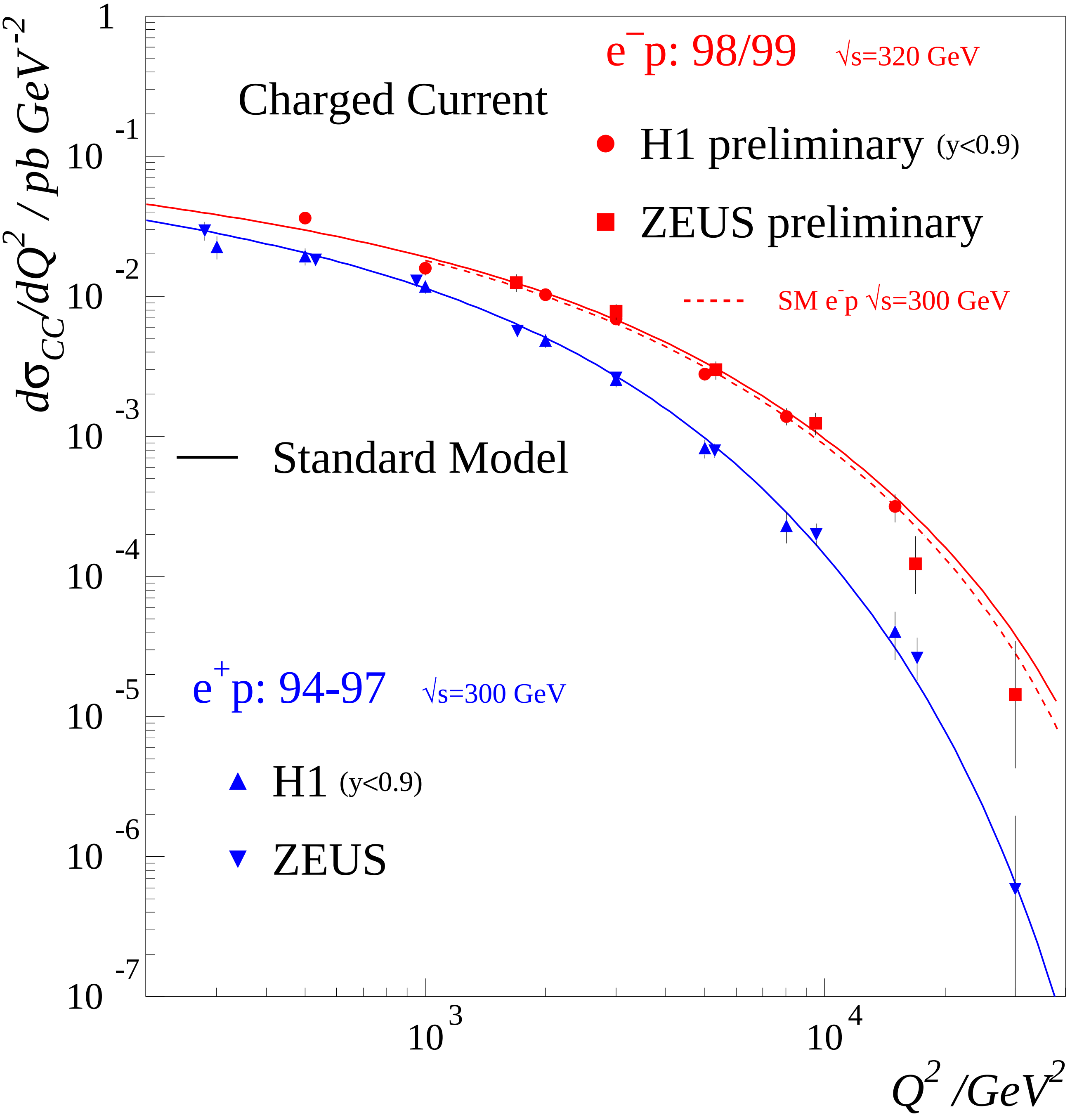

At large Q^2,

e^-p data an order of magnitude above e^+p,

since $\sigma_{e^-p} \propto u$

while $\sigma_{e^+p} \propto (1-y)^2 \cdot (d+s)$

W propagator mass from $d\sigma^{CC}/dQ^2$

$$\frac{d^2\sigma_{CC}}{dxdQ^2} = \frac{G_{CC}^2}{2\pi x} \cdot \left[\frac{M_{prop}^2}{Q^2 + M_{prop}^2} \right]^2 \cdot \Phi(x, Q^2)$$

where: normalisation given by coupling (G_{CC})
shape given by propagator mass (M_{prop}) dependence

Notice: we measure the propagator (i.e. spacelike W) mass, complementary to e^+e^- and pp timelike measurements

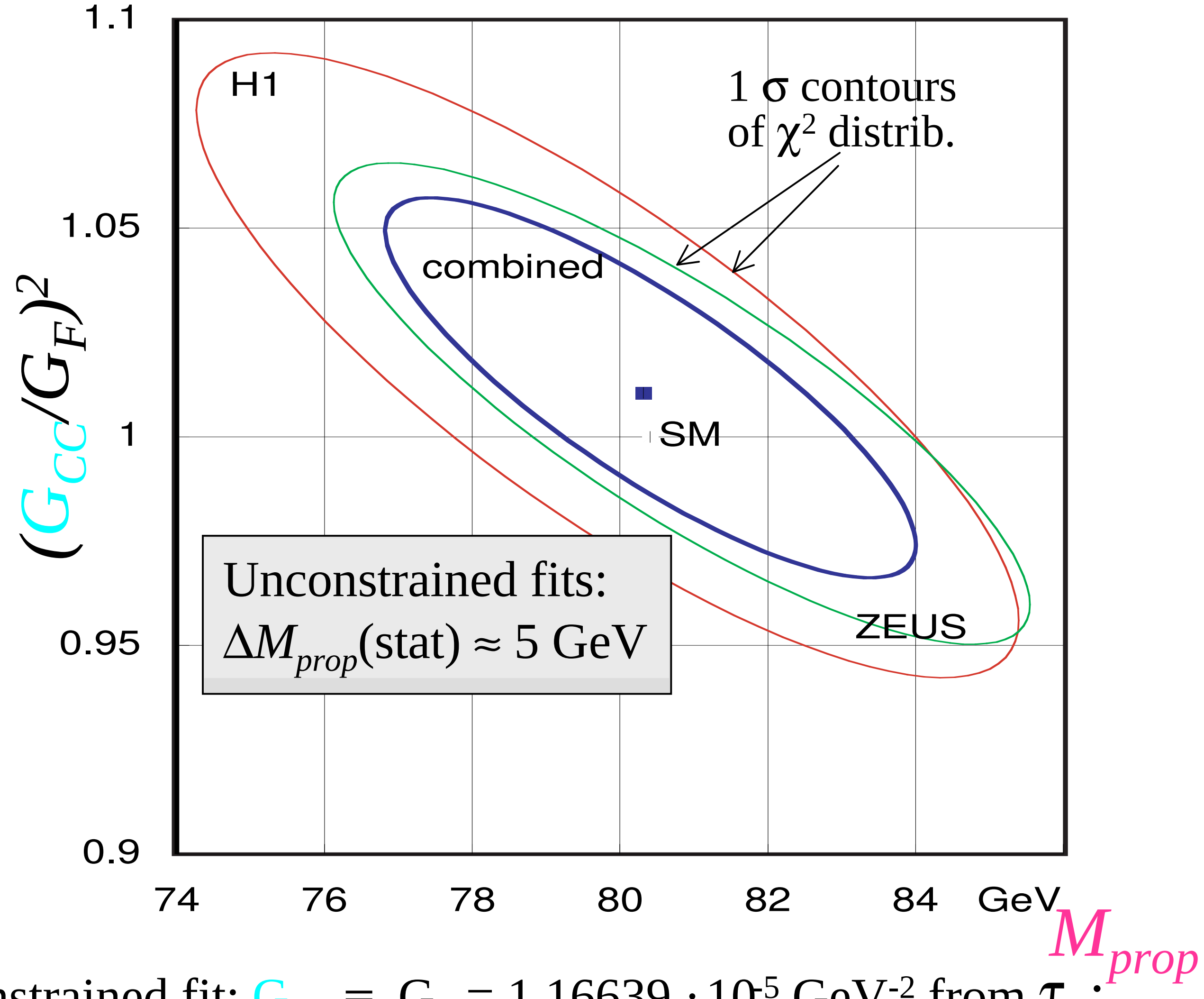

Constrained fit: $G_{CC} \equiv G_F = 1.16639 \cdot 10^{-5}\ \mathrm{GeV}^{-2}$ from τ_μ:

$$M_W = 81.4^{+2.7}_{-2.6}(stat) \pm 2.0(syst)^{+3.3}_{-3.0}(pdf)\ GeV$$ ZEUS

$$M_W = 80.9 \pm 3.3(stat) \pm 1.7(syst) \pm 3.7(pdf)\ GeV$$ H1

⇒ no evidence for anomalous space-like EW sector.

W propagator mass from $d\sigma^{CC}/dQ^2$

ZEUS uses SM relation: $G_F = \dfrac{\pi\alpha}{\sqrt{2}} \dfrac{M_Z^2}{M_W^2(M_Z^2 - M_W^2)} \dfrac{1}{1-\Delta r(M_W)}$

to exploit strong dependence of normalisation (G_F) on shape (M_W) in a model dependent fit: the 3% cross section uncertainty is cast in the uncertainty of a single electroweak parameter.

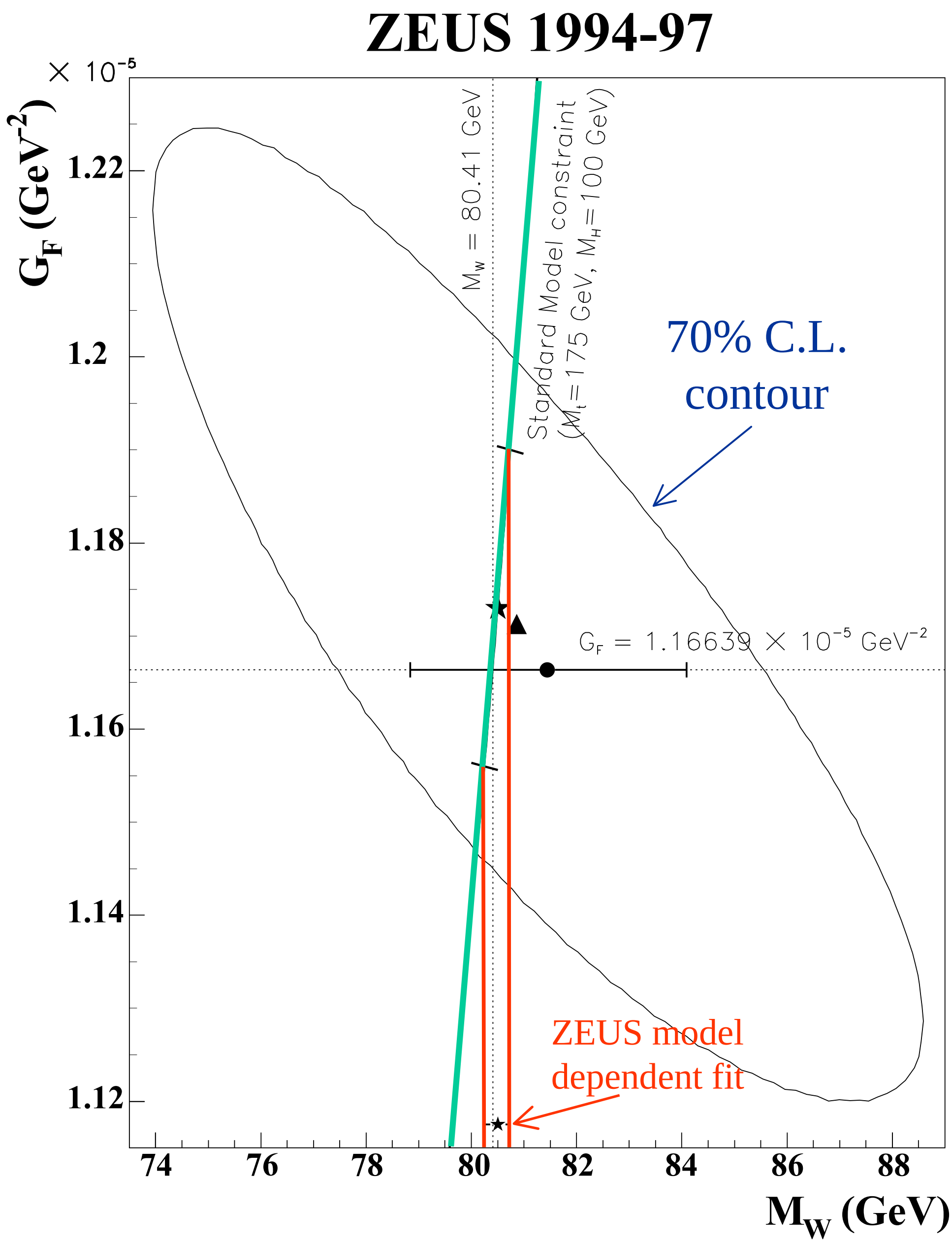

ZEUS: extract M_W at M_H = 100 GeV, M_T = 175 GeV

$$M_W = 80.50^{+0.24}_{-0.25}(stat)^{+0.13}_{-0.16}(syst) \pm 0.31(pdf)^{+0.03}_{-0.06}(M_T, M_H, M_Z)\,GeV$$

(PDG: M_W = 80.39 ± 0.04 GeV)

NC and CC e$^-$p Cross Sections

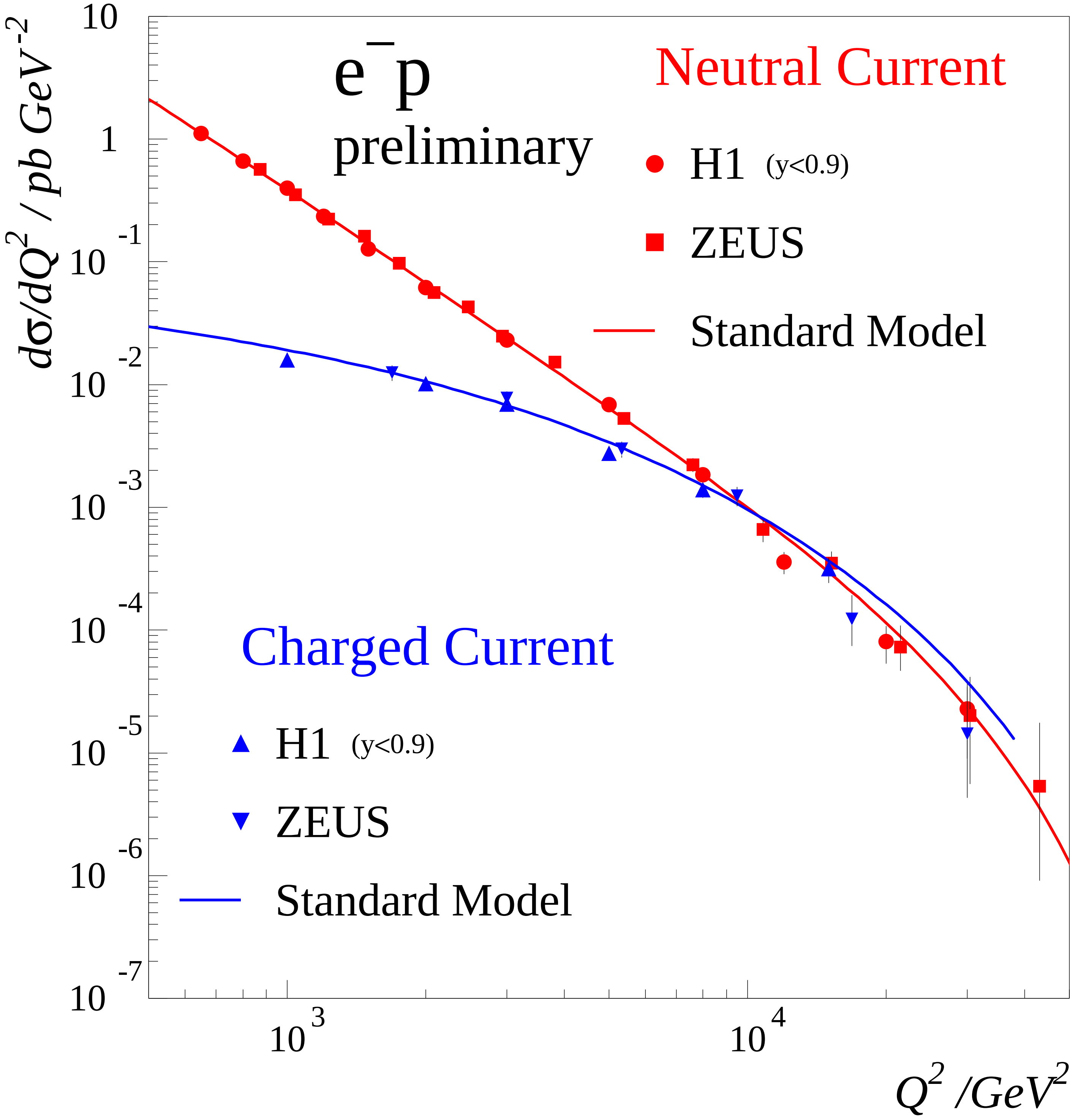

Unification of charged and neutral currents!

HERA Luminosity Upgrade

- HERA reached
  instantaneous Luminosity of 1.4×10^{31} cm^{-2} s^{-1}
  close to design value
  $\Rightarrow$ delivered ~ 45 pb^{-1} to each experiment in 1999.

- The physics done so far is "low Q^2-physics"
  compared to the electroweak scale $Q^2 \approx M^2_W$
  HERA was built to explore.

$\Rightarrow$ NEED FOR:

1. LUMI UPGRADE

2. e-POLARISATION

- The unique features of HERA, like
  e-polarization and e^+ vs. e^- running,
  are relevant only in the EW regime.

- At these large scales new
  phenomena outside the Standard Model
  are more likely to appear.

HERA Luminosity Upgrade

Goal: increase, in the year 2001, the instantaneous luminosity **from 1.5 $\cdot 10^{31}$ to 7.5 $\cdot 10^{31}$ cm^{-2} s^{-1}** by:

- Stronger focusing of e and p beams closer to interaction point
- Installing focusing/separating magnets inside detector volume
  (QO, QG, BG: superconducting magnets
  QI: normal conducting magnet)

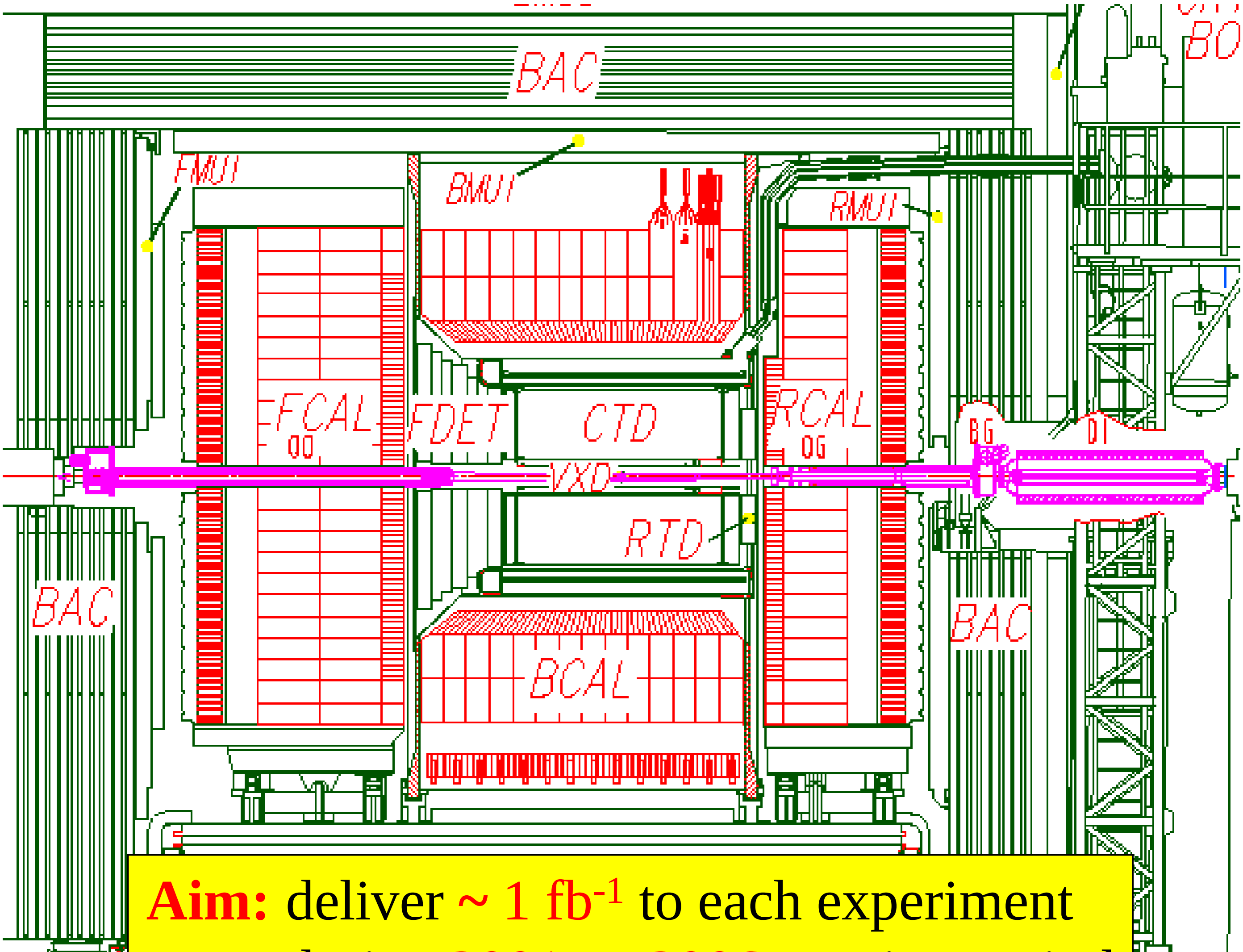

Aim: deliver ~ 1 fb^{-1} to each experiment during 2001 → 2006 running period

In addition, install spin rotators to have **longitudinally polarised e$^{\pm}$ beams**

Future Physics at HERA

Examples:

→ simulation of the proton structure function F_2 obtainable with 1 fb^{-1} at HERA:

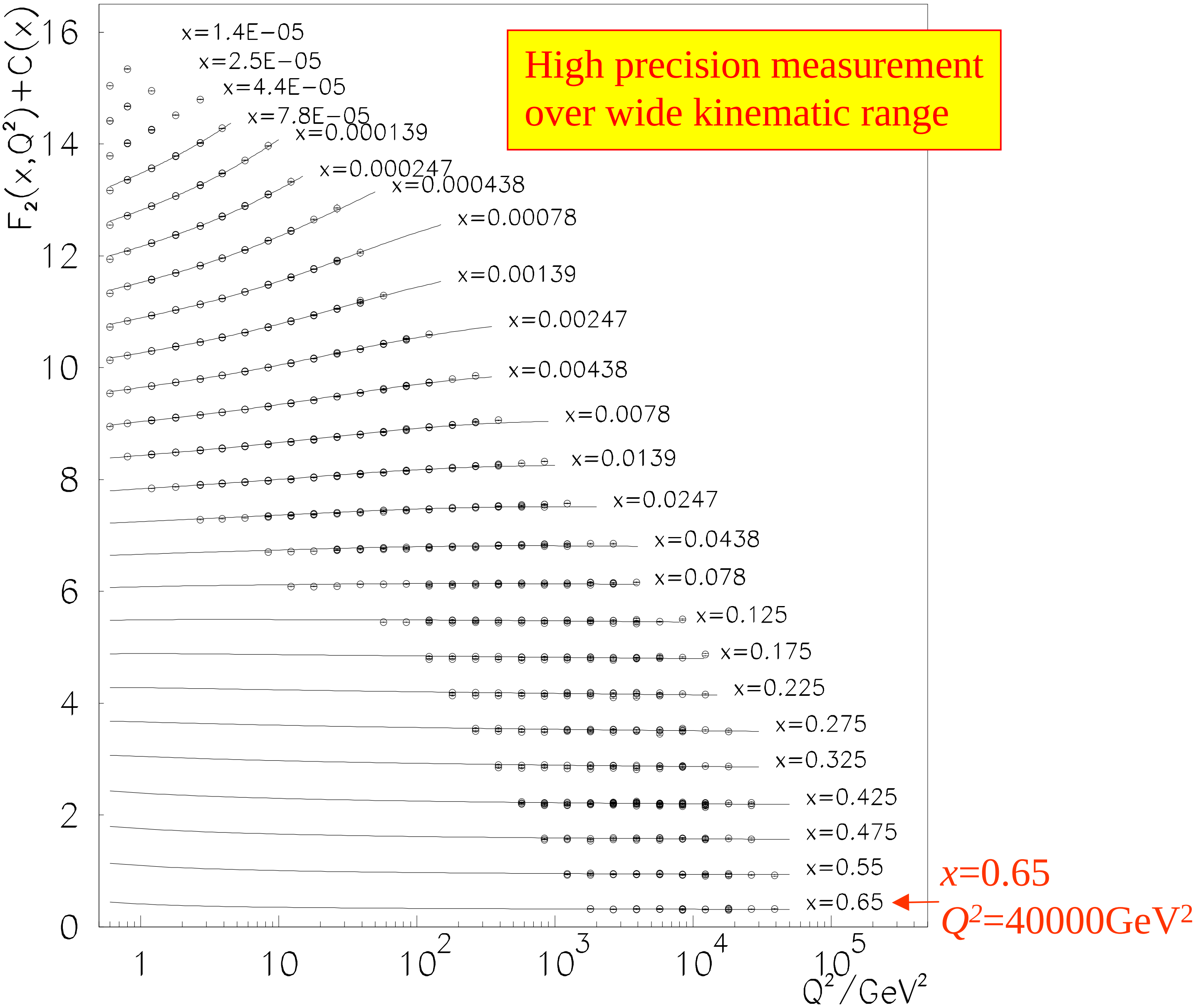

- Stringent tests of QCD evolution equations
- Important expt. input for future hadron colliders
- Experimental precision level:
  - 0.001 on $\alpha_s(M_{Z^0})$ (HERA + fixed target)
  - 1% on gluon density extraction

Future Physics at HERA

Examples:

→ New Physics: – Rp violating SUSY
– lepton flavour violation
– excited fermions

In many instances HERA already sets the best limits. Large luminosity increase would further enhance the sensitivity.

→ e-polarisation:

Standard Model:

$SU(3) \otimes SU(2)_L \otimes U(1)$

observation of charged current interactions with e^-_R or e^+_L beams would imply exchange of W_R

⇒ new interaction

$\nu_R \equiv N_{Majorana} \Rightarrow$ massive

$1fb^{-1} \Rightarrow$ sensitive to M_N ~150 GeV.

Spectacular experimental signature:

$N \rightarrow W^{\pm}e^{\mp} \Rightarrow \mathbf{e^{\pm}_{in}} \rightarrow \mathbf{e^{\mp}_{out}}$

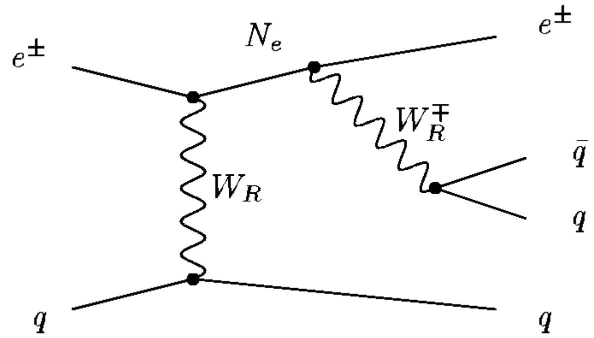

Summary

Structure Functions:

- precision (few %) approaching fixed target data
- F_2 data at lowest ever x-Q^2 (x=10^{-6}, Q^2=0.045 GeV^2) can be described by Regge parameterisations
- DGLAP evolution ok down to $Q^2 \approx 1$ GeV^2 F_2 rise at small x,Q^2 seems driven by Sea quarks
- F_2^{charm} grows up to ~ 25% of F_2
- indirect measurement indicates: $F_L \sim F_L^{QCD}$

Cross sections at large Q^2:

- SM predictions for NC and CC cross sections agree with measurements; need more lumi to constrain PDF's at large x,Q^2
- W-propagator mass consistent with timelike-W mass measurements
- γ–Z interference seen in NC
- unification of Neutral & Charged currents measured

Perspectives:

HERA high luminosity programme:

deliver ~ 1 fb^{-1} during 2001$\rightarrow$ 2006